Event-Based Climatology and Typology of Fog in the New York City Region

ROBERT TARDIF

Research Applications Laboratory, National Center for Atmospheric Research, and Department of Atmospheric and Oceanic Sciences, University of Colorado, Boulder, Colorado*

ROY M. RASMUSSEN

Research Applications Laboratory, National Center for Atmospheric Research, Boulder, Colorado*

(Manuscript received 6 March 2006, in final form 3 November 2006)

ABSTRACT

The character of fog in a region centered on New York City, New York, is investigated using 20 yr of historical data. Hourly surface observations are used to identify fog events at 17 locations under the influence of various physiographic features, such as land–water contrasts, land surface character (urban, suburban, and rural), and terrain. Fog events at each location are classified by fog types using an objective algorithm derived after extensive examination of fog formation processes. Events are characterized according to frequency, duration, and intensity. A quantitative assessment of the likelihood with which mechanisms leading to fog formation are occurring in various parts of the region is obtained. The spatial, seasonal, and diurnal variability of fog occurrences are examined and results are related to regional and local influences. The results show that the likelihood of fog occurrence is influenced negatively by the presence of the urban heat island of New York City, whereas it is enhanced at locations under the direct influence of the marine environment. Inland suburban and rural locations also experience a considerable amount of fog. As in other areas throughout the world, the overall fog phenomenon is a superposition of various types. Precipitation fog, which occurs predominantly in winter, is the most common type. Fog resulting from cloud-base lowering also occurs frequently across the region, with an enhanced likelihood in winter and spring. A considerable number of advection fog events occur in coastal areas, mostly during spring, whereas radiation fog occurs predominantly at suburban and rural locations during late summer and early autumn but also occurs during the warm season in the coastal plain of New Jersey as advection–radiation events.

1. Introduction

Poor visibility associated with the presence of fog represents a hazard to aviation, marine, and road transportation worldwide (Croft 2003). Because of safety concerns, fog occurrences are associated with disruptions in air traffic at airports and navigation in marine ports. Unforeseen reductions in airport capacity associated with reduced ceiling and visibility lead to significant cost increments to the large air carriers. Valdez (2000) concluded that more accurate forecasts of cloud ceiling or visibility with a 30-min lead time would reduce the number of weather delays by 20%–35%. On a national scale, such reductions could save between $500 and $875 million annually. The study by Wilson and Clark (1997) shows daily cost benefits of $100,000–$1,000,000 associated with accurate forecasts of onset and dissipation of stratus clouds and fog. Allan et al. (2001) found that timely forecasts of changes in ceiling or visibility could lead to savings of $500,000 per event at the busy air terminals in the New York City (NYC), New York, area. For the general aviation community, fog is a major safety concern because accidents often occur in reduced visibility conditions (Whiffen 2001). Fog also contributes to creating hazardous conditions on the roads, as evidenced by the numerous multivehicle accidents occurring each year under poor visibility conditions (Whiffen et al. 2003). These are exacerbated in complex urban environments.

Advances in the understanding of the physics of fog have been made through numerous field experiments

* The National Center for Atmospheric Research is sponsored by the National Science Foundation.

Corresponding author address: Robert Tardif, National Center for Atmospheric Research, Box 3000, Boulder, CO 80301.
E-mail: tardif@ucar.edu

DOI: 10.1175/JAM2516.1

(Taylor 1917; Roach et al. 1976; Choularton et al. 1981; Meyer et al. 1986; Findlater et al. 1989; Fitzjarrald and Lala 1989; Duynkerke 1991; Fuzzi et al. 1998) and modeling studies (Lala et al. 1975; Turton and Brown 1987; Ballard et al. 1991; Bott 1991; Golding 1993; Bergot and Guédalia 1994; Teixeira 1999; Nakanishi 2000; Pagowski et al. 2004; Koračin et al. 2005; Thompson et al. 2005). Most of these studies focused on a single type of fog, either radiation or sea (advection) fog. Therefore, a complete understanding of the processes influencing the life cycle of fog in its numerous forms remains elusive. This is particularly true for fog occurring in areas characterized by a complex environment. One such region is the West Coast of the United States, where sea fog has been studied extensively [see Leipper (1994) and listed references therein, as well as the more recent work of Koračin et al. (2001), Lewis et al. (2003), Koračin et al. (2005), and Thompson et al. (2005)]. The complex coastline and topography, variations in land surface characteristics, and high levels of pollution provide a wide range of influences that can potentially affect the dynamical behavior (Fitzjarrald and Lala 1989; Sachweh and Koepke 1997) and microphysical characteristics of fog (Goodman 1977; Hudson 1980; Bott 1991). [See also the online University Corporation for Atmospheric Research/Cooperative Program for Operational Meteorology, Education and Training (UCAR/COMET) modules for comprehensive discussions on factors affecting fog (http://www.meted.ucar.edu/topics_fog.php).]

The NYC region, located on the eastern seaboard of the United States, is another fog-prone coastal region with similar physiographic complexities (complex coastline; presence of urban, suburban, and rural areas; valleys; and rivers and lakes) and with significant variability in aerosols (Ito et al. 2004). However, fog in that part of the United States has not been studied as extensively as on the West Coast. George (1940) performed pioneering work on the identification of fog-inducing mechanisms and associated weather regimes for several locations in the eastern and southern United States, with one location in the general vicinity of NYC. Fitzjarrald and Lala (1989) and Meyer and Lala (1990) studied boundary layer mechanisms and climatological parameters associated with radiation fog for a location in the Hudson Valley, north of NYC. More recently, Croft and Burton (2006) examined the relationship between the extent of fog and the various synoptic weather patterns during a single winter season in the northern mid-Atlantic part of the United States. Other studies provide general annual (Peace 1969) and monthly (Hardwick 1973) fog frequencies at the national scale, while others have attempted to provide a general indication of the geographical distribution of dominant fog types (Willett 1944; Byers 1959; Pettersen 1969). These studies do not provide a level of detail sufficient enough to identify either the mechanisms influencing the formation of all forms of fog or their space–time variability at the regional scale.

The goals of the work presented herein are the identification and classification of fog events into specific types that reflect the primary mechanism responsible for their formation in the complex environment of the NYC region.[1] The characterization of the spatial and temporal variability of fog is also an objective. This approach is deemed more insightful than general station climatologies because it provides specific information about the distribution (spatial and temporal) of fog-forming mechanisms. The approach provides an alternative to the synoptic classification approach (e.g., Croft and Burton 2006) by focusing on the local-scale aspects of fog formation rather than on large-scale weather patterns. The characterization of the associated large-scale weather patterns and other influences follows naturally once specific fog types have been identified, as shown by Meyer and Lala (1990). The analysis of large-scale weather patterns and other environmental conditions associated with fog events for each fog type will be the subject of future efforts.

Section 2 presents the dataset used in this study and the various analysis procedures used to identify and characterize fog events. The overall character of fog is described in section 3, and section 4 contains an analysis of the character of the various fog types. A discussion is presented in section 5, and conclusions are outlined in section 6.

2. Dataset and analysis procedure

a. Datasets

The main surface data used in this study are from the National Oceanic and Atmospheric Administration Techniques Development Laboratory Surface Hourly Observations dataset (National Center for Atmospheric Research 2006). These are complemented by data from a buoy located south of Long Island to characterize offshore conditions during specific fog events. Hourly land surface observations of visibility, temperature, dewpoint temperature, wind speed and direction, ceiling height, cloud cover, coded obstruction to vision, and precipitation type and intensity, covering the pe-

[1] This work is in support of a project funded by the Federal Aviation Administration focused on the improvement of forecasts of low cloud ceiling and reduced visibility (fog) occurrences at New York City's airports.

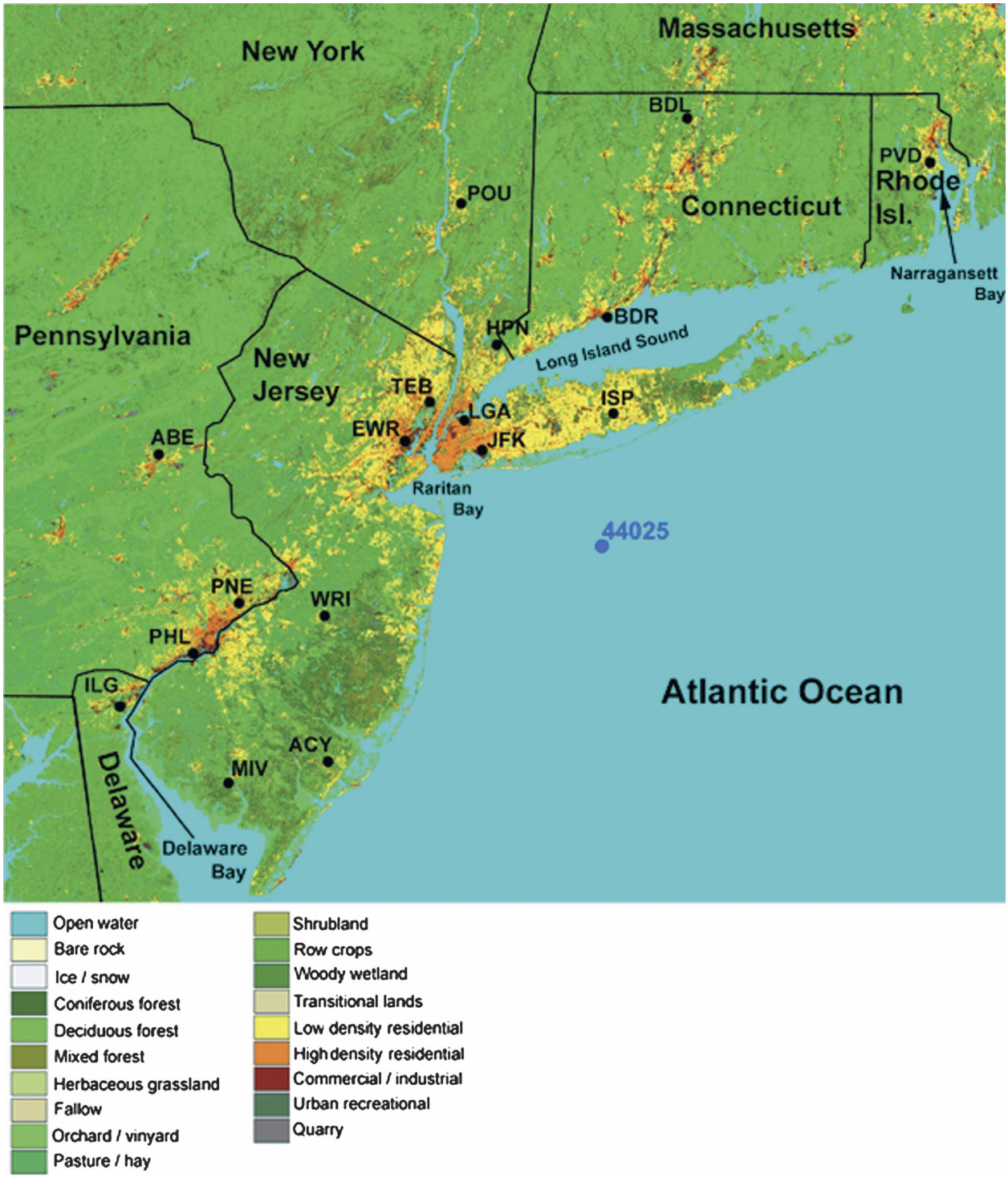

FIG. 1. Map showing the land use of a region centered on New York City, as well as the locations of the 17 land surface stations and the buoy (44025) used in this study.

riod from 1977 to 1996, are used to identify and characterize fog events. This dataset contains data from a period of homogeneous reporting practices, before the introduction of automated weather stations.

Stations were selected such that the main physiographic characteristics of a region centered on NYC are represented. Figure 1 shows a map of surface characteristics (land use) and the location of the sta-

TABLE 1. List of stations, their position, elevation, and physiographic character; and data availability for the 1977–96 study period.

Station code	Station name	Lat (°)	Lon (°)	Elev (m)	Station character	Data availability (%)
EWR	Newark, NJ	40.68N	74.17W	7	Urban–coastal	91.7
JFK	John F. Kennedy Airport, NY	40.65N	73.78W	9	Urban–coastal	94.2
LGA	LaGuardia Airport, NY	40.77N	73.88W	11	Urban–coastal	92.2
ISP	Islip/MacArthur Airport, NY	40.78N	73.10W	43	Suburban–coastal	93.3
TEB	Teterboro, NJ	40.85N	74.00W	7	Urban–inland	90.2
HPN	White Plains, NY	41.07N	73.70W	121	Rural–coastal	89.3
POU	Poughkeepsie, NY	41.63N	73.80W	46	Rural–inland	92.2
BDR	Bridgeport, CT	41.17N	73.10W	7	Suburban–coastal	71.8
BDL	Hartford, CT	41.93N	72.60W	60	Rural–inland	92.7
PVD	Providence, RI	41.73N	71.40W	16	Urban–coastal	93.2
ABE	Allentown, PA	40.65N	75.40W	114	Suburban–inland	93.5
WRI	McGuire AFB, NJ	40.02N	74.60W	41	Rural–inland	91.4
PNE	North Philadelphia, PA	40.08N	75.00W	28	Suburban–inland	86.5
PHL	Philadelphia, PA	39.88N	75.20W	18	Urban–inland	93.4
ACY	Atlantic City, NJ	39.45N	74.50W	23	Suburban–coastal	93.5
MIV	Millville, NJ	39.37N	75.00W	23	Rural–coastal	91.2
ILG	Wilmington, DE	39.67N	75.60W	28	Suburban–inland	93.7

tions. Table 1 provides information about each station's position, elevation, and physiographic character, which is defined by the proximity to coastlines (coastal or inland) and the density of buildings in the vicinity (urban, suburban, or rural). Coastal stations are located within 20 km of the Atlantic Ocean, Long Island Sound, Raritan Bay, Narragansett Bay, or Delaware Bay. Distances between inland stations and coastlines range from approximately 30 (TEB from the Long Island Sound and Raritan Bay) to roughly 140 (ABE from the New Jersey shoreline) km. Other inland stations are located 70–80 km away from the coast. Urban stations are found in high-density residential, commercial, or industrial areas, while suburban stations are located in low-density residential areas. Stations in remote areas away from major urban centers are labeled as rural.

Most stations are located on locally flat terrain with elevations within 50 m of sea level (Table 1). Nevertheless, stations are found in areas with diverse topographical features. Stations are found in valleys such as the Hudson Valley (POU), Connecticut River Valley (BDL), and Lehigh Valley (ABE) (Fig. 2). Coastal areas in the extreme southern portion of New York and Connecticut are characterized by terrain slightly sloping upward away from the coast with an elevation increase of about 10 m km^{-1}. The highest station in the region (HPN) is therefore under the influence of a slight upslope flow during onshore wind conditions. Stations are also found in the coastal plain of southern New Jersey (MIV, ACY, and WRI) and in the plain along the Delaware River (ILG, PHL, and PNE). EWR and TEB are located on flat land with nearby sharp topographical features approximately 150 m in height, such as the Palisades east of TEB and the Watchung Mountains to the west of EWR. Other stations are located on the flat terrain of the Atlantic coastal plain.

Stations reporting during the whole diurnal cycle and with a high ratio of valid visibility observations to the maximum possible number of hourly observations were retained. Only stations with 90% or more valid observations were kept for the analysis, with the exception of BDR, which had about 72% data availability. Because missing records occurred randomly in time (seasonally and diurnally) at this station, it was retained in order to have a location representing the marine environment on the northern coast of the Long Island Sound. Other stations located along the Long Island Sound did not have sufficient annual coverage during the 1977–96 period to be included in the analysis. This selection criterion is used to ensure adequate temporal coverage needed for the reliable identification of fog events. Because in many cases fog is a nocturnal phenomenon, stations that only reported daytime observations were inadequate. The limited number of remaining stations results in some gaps in the dataset's spatial coverage and a possible lack of representation of other geophysical influences, such as the possible enhanced nocturnal cooling associated with the sandy soil of the Pine Barrens found in southern and central New Jersey as well as in eastern Long Island. Nevertheless, the diversity of the physiographic character of the stations provides a representation of most of the influences believed to affect fog occurrences in the region, such as land–sea contrasts, land surface variability (urban, suburban, and rural areas), and topography.

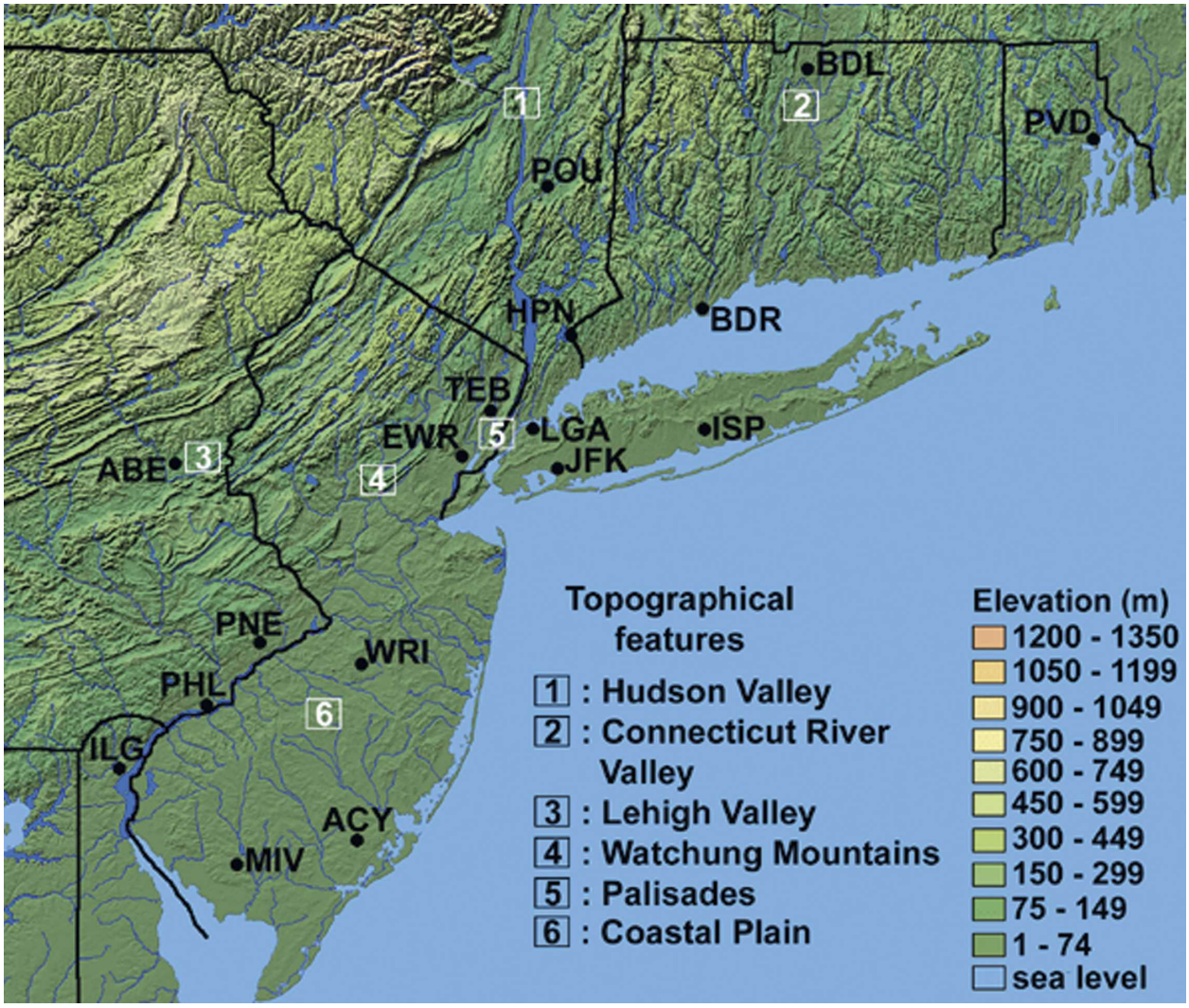

FIG. 2. Shaded relief map of the region centered on New York City, showing the locations of the 17 land surface stations and noteworthy physiographic features.

b. Analysis procedure

1) IDENTIFICATION OF FOG EVENTS

The international definition of fog is an observed horizontal visibility below 1 km (5/8 mi.) in the presence of suspended water droplets and/or ice crystals (National Oceanic and Atmospheric Administration 1995). However, authors have used various definitions depending on the focus of their studies. Heavy fog conditions with visibilities reduced to a few hundred meters or less are a hazard for motorists on the roads, while aviation safety is impacted by less severe reductions in visibility. A threshold of 400 m was used by Peace (1969), Hardwick (1973), Meyer and Lala (1990), and Westcott (2004). Friedlein (2004) defined dense fog as a visibility equal to or below 500 m (5⁄16 mi.), while Croft et al. (1997) set a defining threshold of 800 m (½ mi.). Cho et al. (2000) used the international definition in their study, while Croft and Burton (2006) used National Weather Service climate summaries to identify days during which fog was observed, regardless of its intensity (visibility reduction) and duration.

Fog occurrences are defined here by using the visibility threshold corresponding to the Low Instrument Flight Rules (LIFR) used in the United States (National Weather Service 2004). The presence of fog is defined as an observed visibility of less than 1.6 km (1 statute mile) with fog, ground fog, or ice fog reported concurrently. The study is therefore consistent with the concerns of aviation forecasters who are tasked with forecasting LIFR conditions, and those of general aviation pilots who are concerned with avoiding such con-

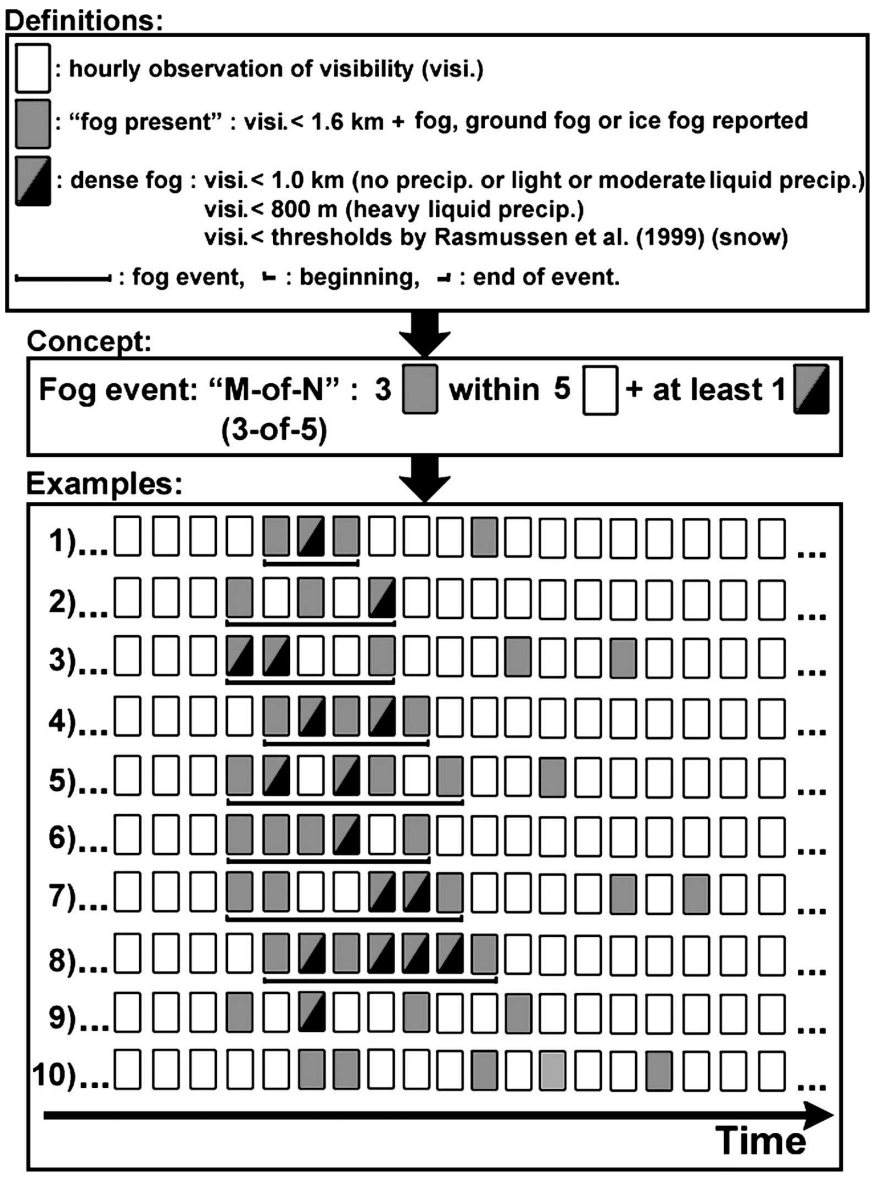

FIG. 3. Diagram illustrating the definitions and concepts used in the identification of fog events in time series of hourly observations of visibility. Examples of fictitious fog events (first eight examples) as well as cases not qualifying as events (last two examples) are shown in the lower part of the diagram.

ditions. The concept of fog *events* at individual stations, defined as well-defined sequences characterized by the presence of fog, is also used. The concept of positive "*M*-of-*N*" constructs (Setiono et al. 2005) is used to identify events, with *M* representing the number of hours with fog within a number of *N* consecutive hourly observations. A negative construct is defined as a sequence of *N* consecutive hourly observations with less than *M* hours with fog. An event begins with the first fog occurrence within a positive construct, and lasts until the first report of the absence of fog part of a negative construct. An additional requirement that one report of dense fog (visibility of less than 1 km) must be present in an event is used to provide consistency with the international definition. The methodology used in identifying events is summarized in Fig. 3, and examples are provided. After a careful inspection of a large number of observations, values of $M = 3$ and $N = 5$ were chosen to define a positive construct. These values were chosen to capture well-defined sequences of fog and eliminate isolated fog occurrences from the analysis. By restricting the analysis to such sequences,

factors influencing the life cycle of fog can be identified with greater confidence as longer-lived conditions are adequately sampled given the resolution of the observational dataset. Adequate sampling and identification of short-term micrometeorological fluctuations are not achievable with hourly surface observations. Although isolated fog occurrences, mostly accompanied by surrounding missing data, are eliminated from the subsequent analysis, 76% of all fog reports are found within the identified events. A closer examination of the isolated occurrences did not reveal a preference with respect to location and season. However, a preference with respect to the time of day was detected. The implications will be discussed in section 4.

2) FOG-TYPE CLASSIFICATION: PRIMARY FOG MECHANISMS

A comprehensive fog-type classification, established by Willett (1928) and later modified by Byers (1959), is composed of 11 fog types based on formation mechanisms and weather scenarios often associated with fog. Citing practical issues, George (1951) proposed a simpler classification of six types. Following George's concerns and recognizing that the use of hourly surface observations imposes inherent limitations on the sophistication of the identification of fog types, the classification used herein relies on broadly defined types. The manual inspection of a considerable number of observations led to the identification of the following five distinct types: *precipitation* fog, *radiation* fog, *advection* fog, fog resulting from the *lowering of cloud base*, and *morning evaporation* fog. Some of these types are part of George's classification (radiation and advection). In contrast to George's classification, advection–radiation fogs are included in the radiation category and no distinction is made between restricted heating and air drainage fogs as radiation fog types. Also, the precipitation fog category is a generalization of George's frontal fog types. The other two types considered here are not part of traditional classifications. However, occurrences of fog resulting from the lowering of cloud bases have long been recognized by researchers and operational forecasters (Petterssen 1940; Peak and Tag 1989; Baker et al. 2002). Morning evaporation fogs are not commonly discussed in the literature, but are included to represent a distinct scenario identified during the inspection of observations.

Several factors may be responsible for fog formation. Advection of temperature and/or moisture can play a role in the formation of radiation fog, and radiative cooling may be a factor in the formation of other fog types. A classification algorithm based on simple conceptual models of fog formation is applied to surface observations of visibility, temperature, wind, precipitation, cloud cover, and ceiling height. It assigns a type of fog for each event identified at individual stations using a series of decision nodes designed to identify the primary mechanism responsible for fog formation. The physical reasoning used to establish the classification of events is summarized in Table 2, while the algorithm's decision process is illustrated with a flowchart in Fig. 4.[2] As in Baars et al. (2003), a number of fog events were randomly selected (representing about 10% of the total number of events) and an independent subjective assessment of the fog type was performed. Associated rules and thresholds were derived based on the evolution of observations during the 5 h prior to onset. The wind speed threshold used to identify radiation fog events has been chosen based on information found in Taylor (1917) and Meyer and Lala (1990). Typical scenarios of observed surface observations associated with each fog type are shown in Fig. 5.

A precipitation fog event is illustrated in Fig. 5a. Overcast conditions were observed at HPN during several hours with obscured conditions in fog reported following a lowering of the cloud base as light rain persisted. Given that the lowering of the cloud base and the decrease in visibility occurred as precipitation was falling, and cooling of the moistened air did not occur, the reasoning is that the evaporation of precipitation played a central role in the formation of fog. A radiation fog event is presented in Fig. 5b. A typical evening transition of the boundary layer occurred under mostly clear skies at WRI during the evening of 29 September 1990. A rapid decrease in the near-surface temperature was followed by a slower cooling rate. Wind speeds at or below 2 m s^{-1} were observed throughout the night. Visibility gradually decreased during the cooling period, leading to obscured conditions in fog at 0600 UTC 30 September. Figure 5c illustrates conditions associated with an advection fog event. A sudden decrease in visibility and appearance of a low ceiling occurred at JFK on 14 May 1992. Visibility dropped sharply from 14 to 0.8 km as a broken cloud cover appeared below 100 m. This transition took place as the wind shifted from a westerly to southerly flow with speeds around 3 m s^{-1}. These conditions are indicative of a fog layer being advected inland from the coastal ocean. A typical cloud-base-lowering scenario is illustrated using observations from MIV on 20 and 21 April 1992 (Fig. 5d). A period of gradual cloud-base lowering took place over a

[2] Fog events that do not meet the criteria used to classify events into the five types, or those for which a condition of insufficient valid data characterizes the few hours prior to fog onset, are classified as *unknown*.

TABLE 2. List of fog types used in the classification algorithm and associated primary mechanisms, as well as definitions based on the morphology of fog formation.

Fog type	Primary physical mechanism	Definition/morphology of fog formation	References
Precipitation (PCP)	Thermodynamical influence of evaporating precipitation	Precipitation observed at the onset of fog or the hour prior	Petterssen (1969)
Radiation (RAD)	Radiative cooling over land	Onset during the night with an observed wind speed below 2.5 m s^{-1} and cooling during the hour prior in absence of a cloud ceiling, or with a cloud base rising concurrently or slight warming in the hour leading to onset if preceded by cooling period (e.g., fog forming between two hourly observations) or cloud ceiling below 100 m if followed shortly by fog at surface (e.g., elevated fog formation)	Taylor (1917), Pilié et al. (1975), Roach et al. (1976), Roach (1995a), Meyer et al. (1986), Meyer and Lala (1990), Baker et al. (2002)
Advection (ADV)	Shear-induced mixing of air parcels of contrasting temperatures as moist, warm air flows over a colder (water, land, or snow) surface	Onset as a "wall" of fog reaches a station, with an observed wind speed greater than 2.5 m s^{-1} and an associated sudden decrease in visibility or sudden appearance of a cloud ceiling below 200 m, followed by fog onset within next 2 h	Roach (1995b), Baars et al. (2003)
Cloud-base lowering (CBL)	Moistening and/or cooling of the layer below boundary layer stratiform clouds and/or prolonged subsidence	Gradual lowering of a cloud ceiling within a 5-h period prior to fog onset, with initial ceiling height below 1 km	Petterssen (1940), Oliver et al. (1978), Pilié et al. (1979), Duynkerke and Hignett (1993), Koračin et al. (2001), Baker et al. (2002)
Morning evaporation (EVP)	Evaporation of surface water and mixing in the surface layer	Increasing temperature and greater increase in dewpoint leading to saturation, within 1 h of sunrise	Arya (2001), Brutsaert (1982)*

* These references do not specifically discuss the formation of fog under the influence of evaporation at sunrise, but rather present comprehensive discussions on the evaporation of water at the earth's surface.

few hours leading to fog conditions at the surface at 0100 UTC 21 April. The cloud-base lowering occurred in the absence of precipitation as gradual cooling of the near-surface temperature took place. Observations at WRI on 14 September 1989 are used to illustrate an event of morning evaporation fog (Fig. 5e). Cooling of the near-surface temperature occurred during the preceding night under varying cloudiness and light wind speeds (<2 m s^{-1}). The visibility remained constant at 11 km until the latter part of the night, when it decreased to values in the 4–5 km range as near-saturated conditions were reached. Visibility dropped to 100 m while temperature warmed by 0.6°C and the dewpoint increased by 1.1°C shortly after sunrise. As this occurred under calm wind conditions, the increase in humidity could not have been the result of advection, but rather the result of evaporation of surface water as the incoming solar radiation provided the necessary energy.

3) FREQUENCY COMPUTATION

The character of each fog type is examined by determining the spatial distribution of the frequency of fog events, as well as the seasonal and diurnal distributions of fog onset and dissipation frequencies. The monthly/diurnal frequency is calculated as

$$F_{m,h} = 100(N_{m,h}/N_{\text{tot}}), \tag{1}$$

where $F_{m,h}$ is the frequency of events beginning (onset) or ending (dissipation) at hour h during month m, $N_{m,h}$ is the number of events that began at hour h in month m, and N_{tot} is the total number of events. The monthly frequency is then the sum

$$F_m = \sum_h F_{m,h}\,, \tag{2}$$

and the hourly frequency is simply

$$F_h = \sum_m F_{m,h}\,. \tag{3}$$

3. General character of fog

The character of fog is first investigated by examining both the number of hours and days per year during

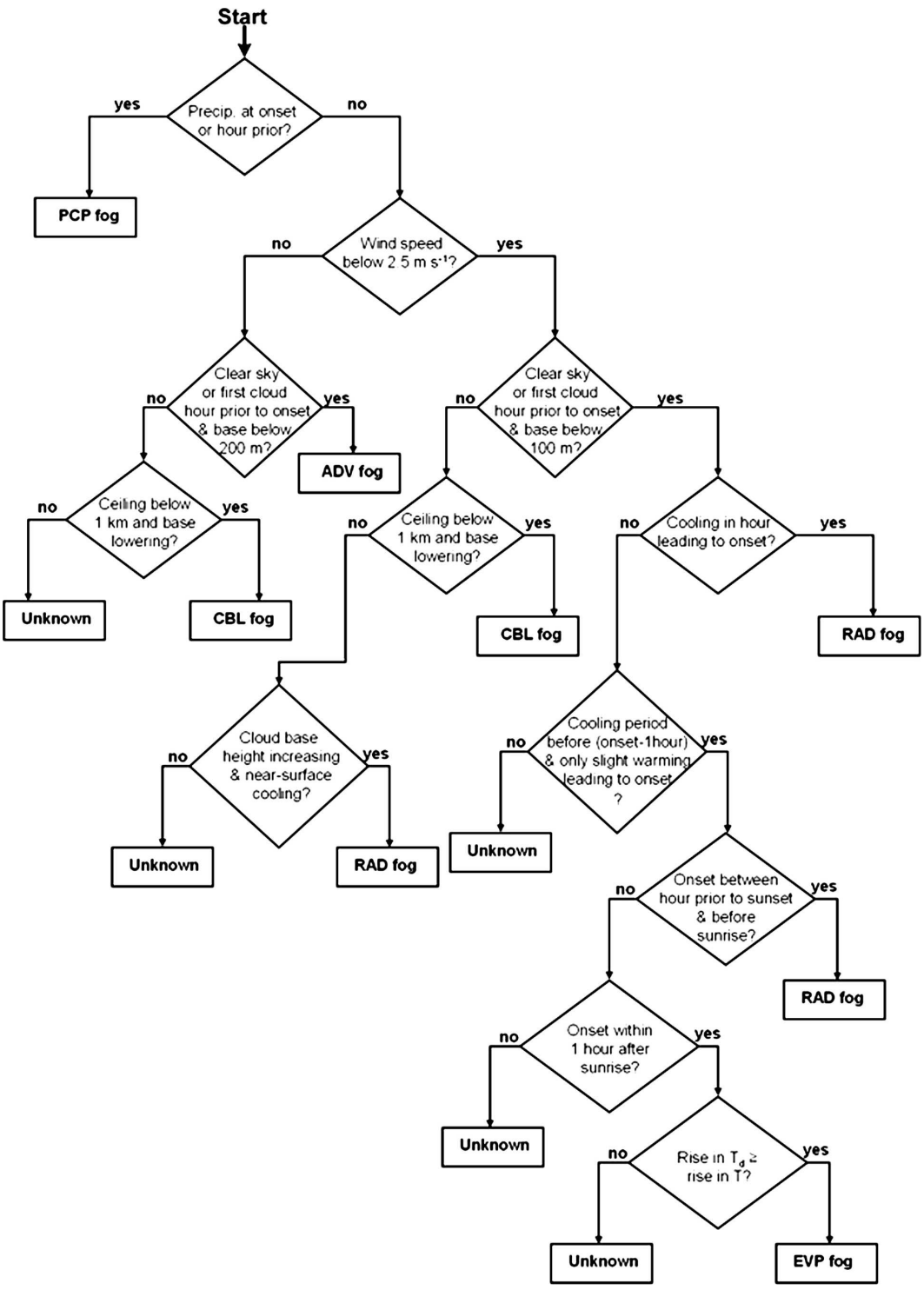

FIG. 4. Flowchart diagram illustrating the fog-type classification algorithm.

which fog conditions defined with various visibility thresholds were observed (Table 3), as well as the number of events that occurred (Fig. 6). The terminology of light (visibility <1.6 km), dense (visibility <1 km), and heavy (visibility <400 m) fog is used. A considerable spatial variability is observed in the number of fog hours and days regardless of fog intensity, as well as in the number of events. This consistency between fog

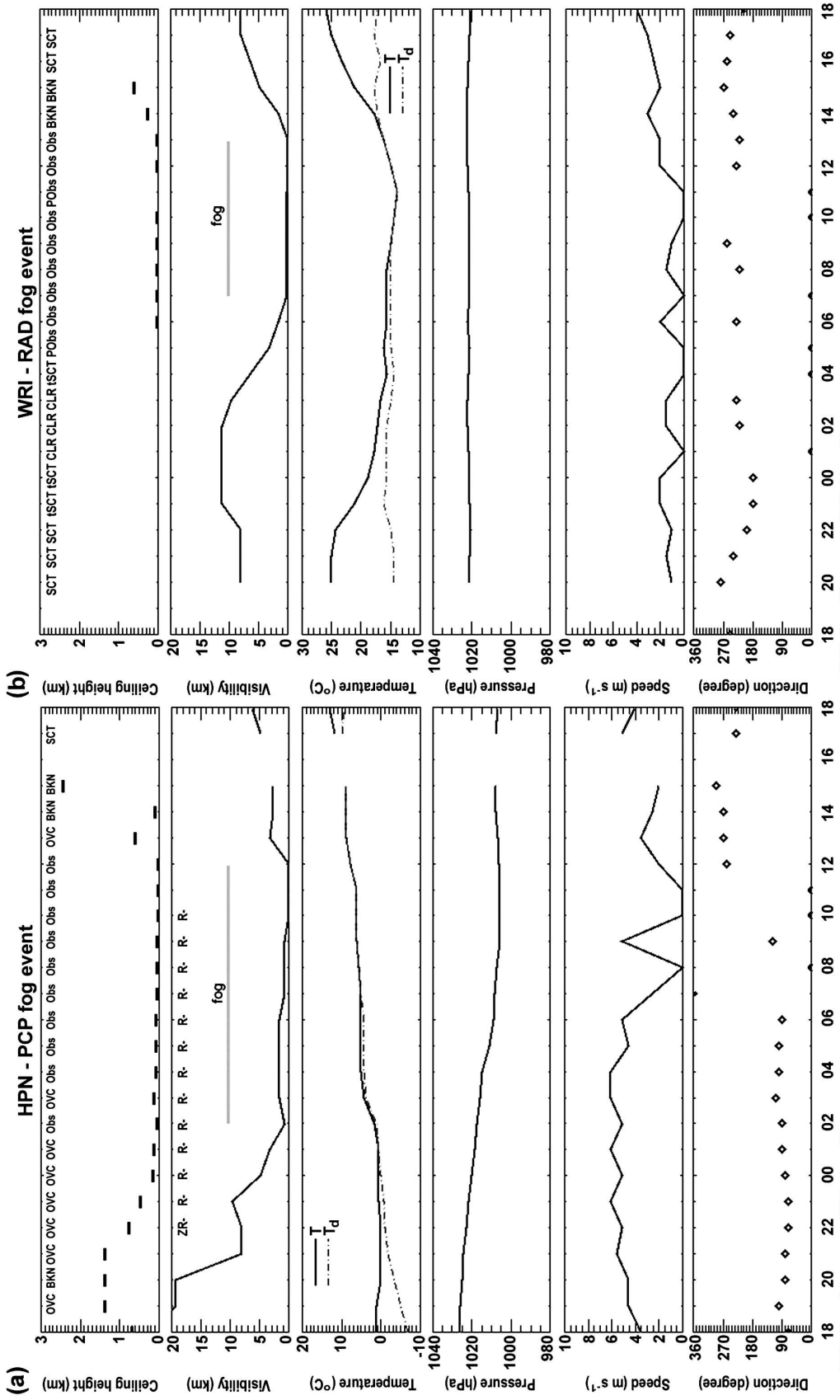

FIG. 5. Example of surface observations associated with (a) a precipitation fog event. Observations were taken at the White Plains airport (HPN) from 1800 UTC 21 Dec to 1800 UTC 22 Dec 1984. (top to bottom) Cloudiness (codes in the upper portion of the top figure) and ceiling heights are represented; visibility and precipitation codes are shown, followed by temperature (solid line) and dewpoint temperature (dashed line), mean sea level pressure, wind speed, and wind direction. The fog period is highlighted with a gray bar in the second panel. (b) Same as (a), but for a radiation fog event that took place at WRI on 29 Sep 1990. (c) Same as (a), but for an advection fog event at JFK on 14 May 1992. (d) Same as (a), but for a cloud-base-lowering fog event at MIV on 21 Apr 1992. (e) Same as (a), but for a morning evaporation fog event at WRI observed on 14 Sep 1989. The arrow in (e) indicates the time of sunrise.

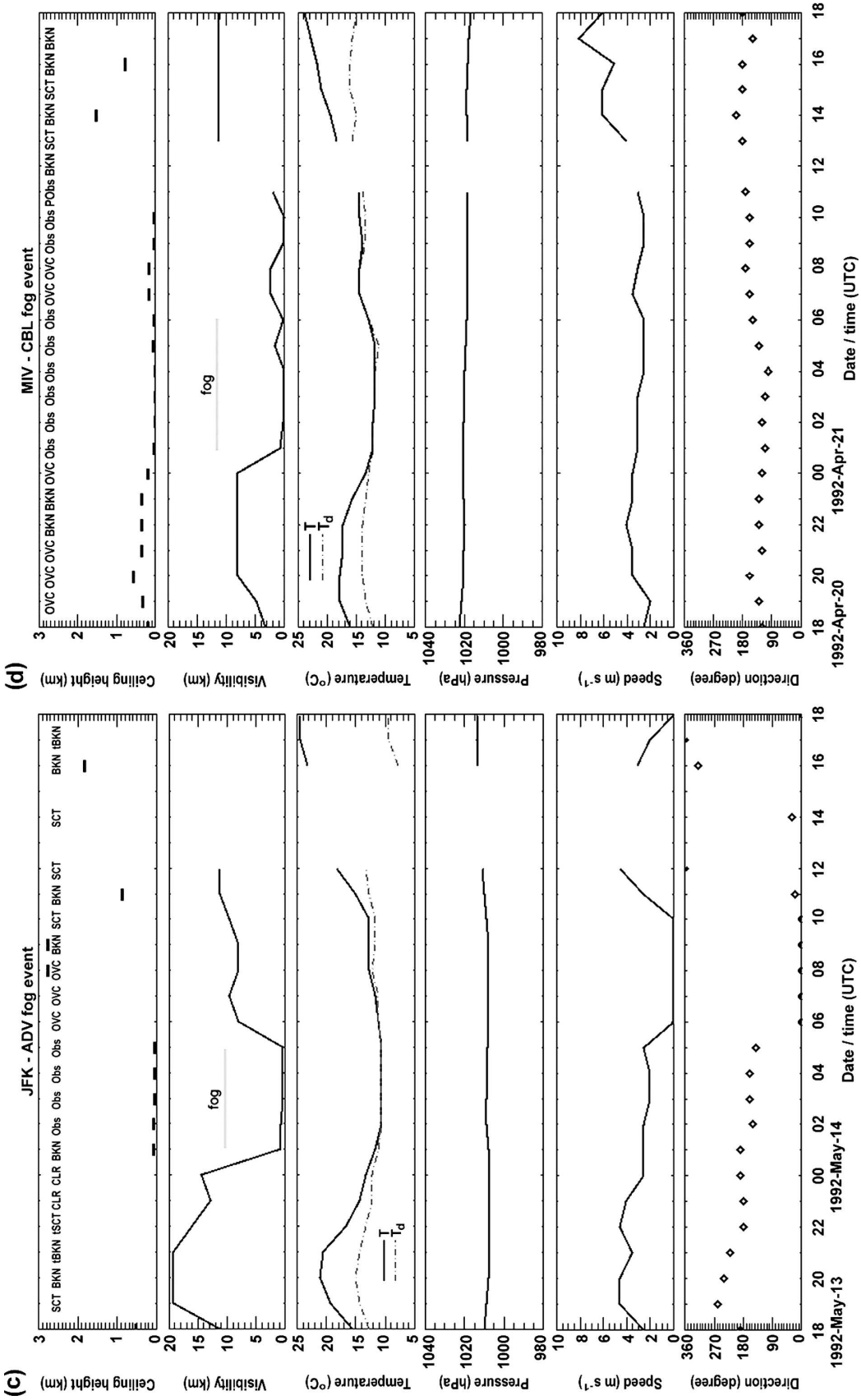

FIG. 5. (*Continued*)

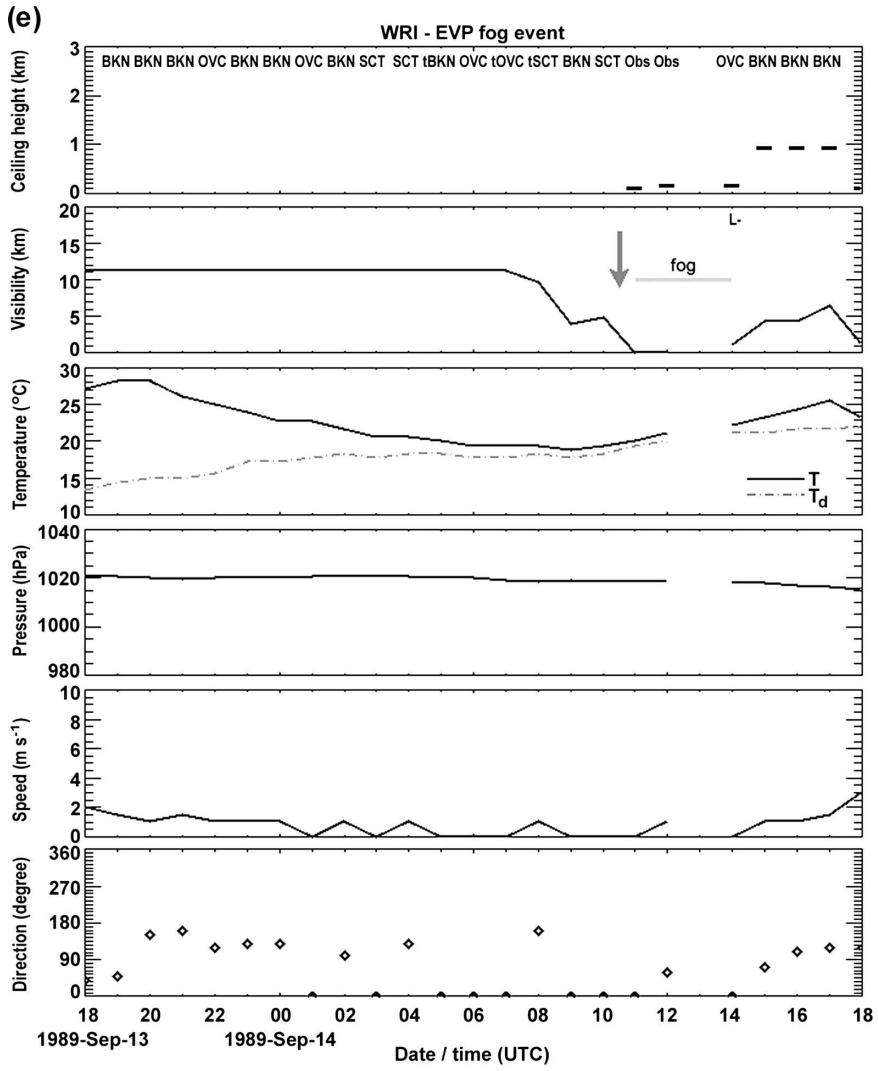

FIG. 5. (*Continued*)

hours and events is not surprising because 76% and 78% of fog (light and heavy, respectively) hours are found within fog events. Overall, coastal suburban and rural locations experience the most fog, followed by the inland rural and suburban stations. Fog is least frequent at urban sites.

More specifically, locations in the urban core of NYC (EWR, TEB, and LGA) rank in the bottom tier with respect to the number of fog hours, days, and events. Also, 20% fewer events were identified at the more urbanized location of PHL relative to nearby suburban PNE. This suggests the urban heat island (UHI) of NYC and Philadelphia, Pennsylvania, has a role in decreasing the likelihood of fog. Previous studies have identified an urban–rural variability in fog (Lee 1987; Bendix 1994) as the result of temperature and humidity contrasts associated with the UHI and related thermal circulations (Sachweh and Koepke 1995, 1997; LaDochy 2005). The presence of an UHI in the New York area is well documented. Bornstein (1968) observed near-surface temperature differences of up to 4°C between the urban core of NYC and its adjacent rural areas at sunrise. Gedzelman et al. (2003) have shown patterns with the warmest nocturnal temperatures in the most urbanized areas of NYC and Philadelphia, which correspond well with the minima in the number of fog hours, days, and events documented in this study.

On the other hand, the HPN and MIV coastal stations stand out as positive anomalies among stations. HPN experiences more than double the number of fog hours, days, and events relative to the respective regional averages over the 17 stations, while MIV has 60% more fog hours and days than the averages thereof

TABLE 3. Number of fog hours and fog days (number in parentheses) per year for fog of various intensities, over the 1977–96 dataset.

Station code	Light fog h (days) (visibility <1.6 km)	Dense fog h (days) (visibility <1.0 km)	Heavy fog h (days) (visibility <0.4 km)
EWR	69 (21)	46 (15)	9 (4)
JFK	176 (41)	149 (37)	51 (16)
LGA	92 (25)	68 (19)	18 (6)
ISP	242 (56)	200 (48)	79 (25)
TEB	79 (26)	47 (17)	12 (5)
HPN	463 (74)	274 (59)	132 (34)
POU	123 (37)	101 (33)	27 (11)
BDR	141 (38)	116 (31)	51 (17)
BDL	156 (41)	114 (32)	37 (13)
PVD	156 (42)	113 (33)	29 (10)
ABE	161 (39)	126 (32)	40 (11)
WRI	208 (53)	149 (39)	60 (18)
PNE	132 (38)	98 (29)	35 (12)
PHL	94 (27)	69 (21)	26 (9)
ACY	226 (53)	192 (47)	75 (22)
MIV	279 (70)	204 (55)	68 (22)
ILG	155 (41)	114 (31)	40 (14)
Average	174 (42)	128 (34)	46 (15)

(Table 3). Stations located directly under the influence of the marine environment (e.g., JFK, ISP, and ACY) and an inland station in the coastal plain of New Jersey (WRI) have among the highest number of fog hours, days, and events. Coastal stations not located on the coastline of the Atlantic Ocean (PVD and BDR) also experience considerable fog. Stations located in suburban and rural inland areas (BDL, POU, ABE, and ILG) show numbers close to the regional averages.

Another noteworthy feature is the contrast in fog occurrences between the nearby coastal stations of JFK and LGA, both of which are located in the urban core of NYC. JFK experiences twice as much fog as LGA. Both locations experience fog onset as mostly onshore flow occurs (not shown). The difference in occurrences may be related to the fact that JFK is located immediately downstream of the open Atlantic Ocean and thus under the direct influence of marine boundary layer air that has traveled long distances over the cold coastal water. In contrast, LGA is located on the northern shore of Long Island and is surrounded by high-density urban neighborhoods, except for a narrow opening on the Long Island Sound. Thus, scenarios for which the station is directly influenced by the marine air are limited.

Light fog conditions are distributed in a manner corresponding to 21–74 fog days yr^{-1} depending on the location within the region, with a regional average of 42 days yr^{-1} (Table 3). Dense fog conditions occurred on 15–59 days yr^{-1} with an average of 34 days yr^{-1}, while heavy fog was reported on 4–34 days yr^{-1} with an average of 15 days yr^{-1}. In comparison with other regions in the United States, Leipper (1994) indicated that 40–60 days yr^{-1} are characterized by heavy fog (visibility <400 m) along the coast of California and Oregon, while Croft et al. (1997) reported 20–50 days of fog with visibilities less than 800 m (½ mi.) for the coastal areas of the Gulf of Mexico. Therefore, while not quite as common as on the West Coast, fog occurrences in the NYC region have frequencies comparable to those of the Gulf Coast. The results are also consistent with those of Peace (1969), which show 20–30 days yr^{-1} of heavy fog for the region investigated in this study. However, the present results indicate a greater regional spatial variability when compared with Peace's coarse analysis.

4. Fog types

a. Fog-type frequency

The fog-type classification algorithm described in Fig. 4 has been applied to every event at each station. A total of 95% of all identified fog events were successfully classified into one of the five types considered. Results indicate that fog formation in precipitation is the most common scenario in the area, with 11 of the 17 stations having their highest proportion of events in this category, and the 6 remaining stations having precipitation fog ranking as the second most likely type (Fig. 7). The overall frequency corresponds to 36% of the totality of events. The common occurrence of fog in precipitation has also been reported by George (1940)

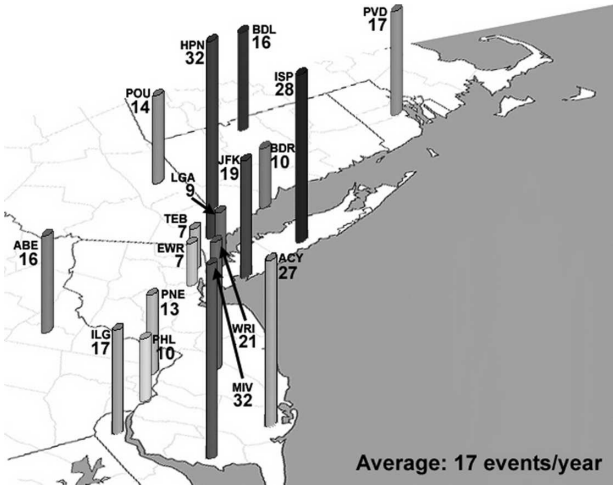

FIG. 6. Average number of fog events per year identified from surface observations taken over the 1977–96 period, for stations located in RI, CT, southern NY, NJ, eastern PA, and northern DE.

for locations in the eastern and southern United States and in the midwestern part of the country by Westcott (2004). Its occurrence in the Piedmont of the Appalachians is also mentioned by Willett (1944). Byers (1959) stated that warm-front precipitation fog in the northeastern United States is among the most frequent in the world because of the presence of polar air masses during winter, which combine with the nearby marine tropical air over the Gulf Stream to create important temperature contrasts in the lower troposphere. Radiation fog is another important component of the overall climatological description with 28% of the events. This fog type occurs most frequently in the suburban and rural areas of the coastal plain of New Jersey, in the valleys of the hilly areas of southern New York, eastern Pennsylvania, and northern Connecticut, and in the plain along the Delaware River. This is in agreement with statements found in Byers (1959) and with the study of Meyer and Lala (1990) characterizing a location in the Hudson Valley. Fog related to the lowering of cloud bases occurs throughout the region, with a frequency of 19% of all events. Ten stations have this type of fog ranking as, or close to, the second most likely fog type. Advection fog is most often observed at locations under the direct influence of the marine environment, representing 9% of all of the events and 17% when only coastal locations are considered. This is in accord with Willett (1944) who pointed out the common occurrence of advection fog in a region extending from the northeast coast to the Newfoundland Grand Banks. Petterssen (1969) also described the Grand Banks advection fog maximum as extending westward with a decreasing frequency along the east coast of the United States. Fog formation related to surface evaporation at sunrise is found to be a relatively minor component in comparison with the other types, with frequencies only up to 5% of all events.

The use of events as a basis for the identification of fog types removes some isolated fog occurrences from the analysis. Results reveal that isolated occurrences are spatially distributed in a manner consistent with the overall fog hours (shown in Table 2). Their monthly distribution is statistically indistinguishable from the one corresponding to the totality of fog hours at the 95% confidence level. However, a clustering of the isolated fog reports occurs in the hour following sunrise, which may suggest that the frequency of morning evaporation fog could be underestimated. When the individual isolated fog reports that match the criteria defining this fog type are included, frequencies increase to 0.5%–8.0%, depending on the location (Table 4). Despite the increase in the number of events, the ranking of this fog type with respect to others remains unchanged. Other isolated fog occurrences could not be preferentially associated with other fog types, mostly because of missing data. Therefore, the relative frequency of fog types based on events can be considered representative of the fog's character in the region.

b. Fog density and duration of events

Parameters of interest in characterizing fog are its intensity expressed as the reduction in visibility and the duration of events. The distributions of event duration compiled over fog events at all stations and over the period covering 1977–96 are shown for each fog type in Fig. 8a. The nonparametric Kruskal–Wallis test (Helsel and Hirsch 1992) is used to test the null hypothesis that all groups of data (event duration for the various fog types) have identical distributions at the 95% significance level. This nonparametric test is used since the requirement for normal distributions does not apply as for the Student's t test. The test was performed on various combinations of groups with results indicating that distributions can be considered statistically different at the 95% confidence level, except when advection and cloud-base-lowering fogs are compared. Fog formation in precipitation has a statistically significant tendency to last the longest, with about 50% of events lasting longer than 8 h and 25% longer than 12 h. A few events (5%) even lasted longer than 29 h. The occurrence of long-lived precipitation events is an important influence on the length of fog events. A good proportion of advection fog events also tends to last a long time, with 25% of the events lasting longer than 10 h. Slow-moving

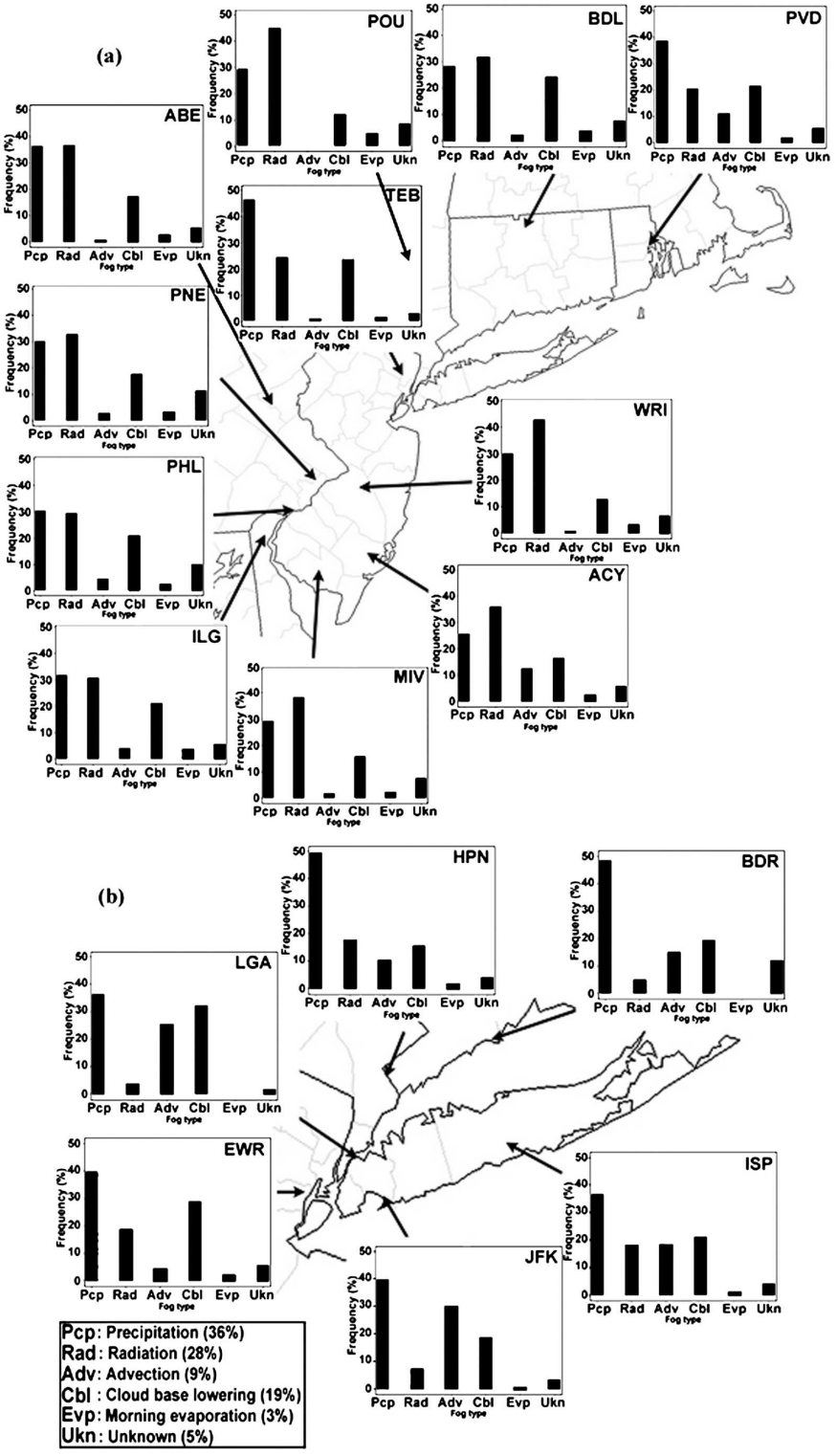

FIG. 7. (a) Frequencies of occurrence of fog types for sites outside of the immediate vicinity of New York City. Frequencies calculated from fog events identified in the dataset between 1977 and 1996 inclusively. (b) Same as (a), but for locations within and in the vicinity of New York City. Total frequencies are indicated in the legend.

TABLE 4. Frequency of morning evaporation fog events and frequencies obtained when considering isolated fog observations matching the criteria defining this type of fog, over the 1977–96 dataset.

Station code	Event frequency (%)	Event frequency + isolated fog reports (%)	Difference
ISP	1.1	1.8	+0.7
JFK	0.3	0.5	+0.2
EWR	2.2	2.9	+0.7
LGA	0.0	1.6	+1.6
TEB	1.5	2.9	+1.4
HPN	1.9	2.6	+0.7
BDR	0.0	3.0	+3.0
POU	4.9	8.0	+3.1
BDL	4.0	4.6	+0.6
PVD	2.1	2.6	+0.5
WRI	3.6	6.2	+2.6
ILG	3.8	4.7	+0.9
ACY	2.7	3.6	+0.9
MIV	2.5	4.0	+1.5
PHL	2.4	5.2	+2.8
PNE	3.4	5.3	+1.9
ABE	2.8	4.6	+1.8

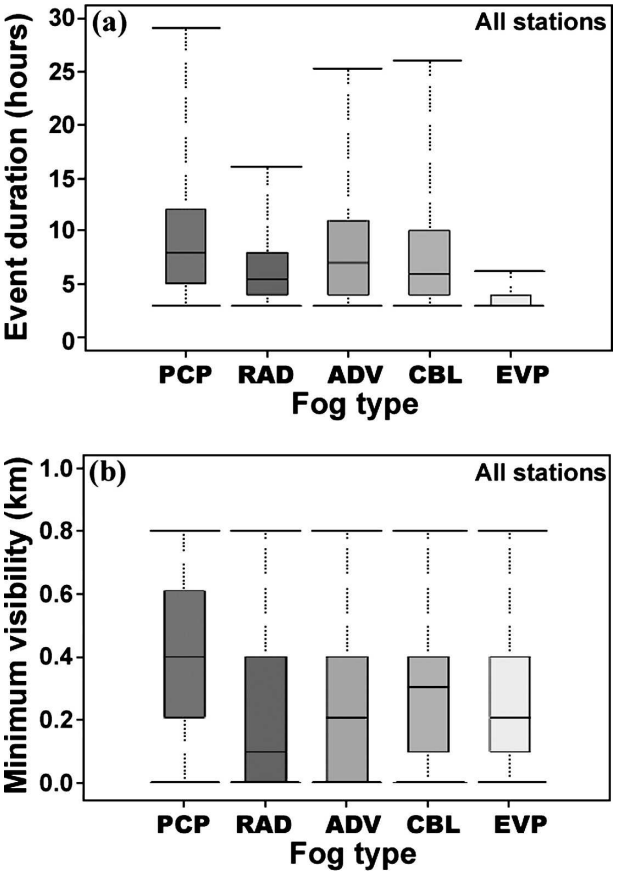

FIG. 8. Distributions of (a) fog event duration and (b) minimum visibility during fog events, for each fog type. Distributions are compiled over all stations, over the 1977–96 period. Distributions are illustrated using box plots, defined using the 5th (lower whisker), 25th (lower edge of box), median (horizontal line within box), 75th (upper edge of box), and 95th (upper whisker) percentiles.

synoptic weather systems driving onshore flows with long trajectories over the cold coastal waters are a factor. Radiation fog events do not last as long, with 75% of the events lasting less than 8 h. As will be shown during the next section, radiation fog onset tends to occur in the second half of the night, limiting the length of its deepening phase. Heating from solar radiation can then quickly dissipate the fog after sunrise. Fog events related to surface evaporation during the morning transition of the surface layer are short lived, as warming begins to dominate over moistening once the surface water has evaporated.

The distributions of minimum visibility observed during fog events of each type have also been tested using the Kruskal–Wallis test. The findings are that the distributions can be considered significantly different from one another at a 95% confidence level. Results reveal similarities as well as differences between fog types (Fig. 8b). Four of the five types have 75% of the events with minimum visibilities in the heavy fog category (below 400 m). Precipitation fog tends to be less dense since one-half of the events are characterized by heavy fog conditions. Radiation fog leads to a greater proportion of heavy fog conditions with half of the events characterized by visibilities at or below 100 m, and 25% of the events with visibilities reduced to zero. Advection fog also produces 25% of the events with obscured conditions, but a smaller proportion of visibilities are found in the 200-m range. Cloud-base lowering and morning evaporation fog events show a smaller proportion of events with minimum visibilities below 100 m.

c. Seasonal and diurnal variability of fog onset

The character of the various types of fog is further illustrated by examining the temporal distributions of fog onset frequencies for each fog type. Frequencies are calculated using Eqs. (1), (2), and (3) applied to events of each type.

Seasonal and diurnal distributions are shown in Fig. 9. Values of $F_{m,h}$ are illustrated with a contour plot in the center panel of each figure, while the hourly and monthly frequencies are shown as histograms in the upper and right panels, respectively. The onset of precipitation fog events is distributed throughout the day with only a slight increase in the nighttime hours (Fig. 9a). Considerable seasonal variability is found, with the

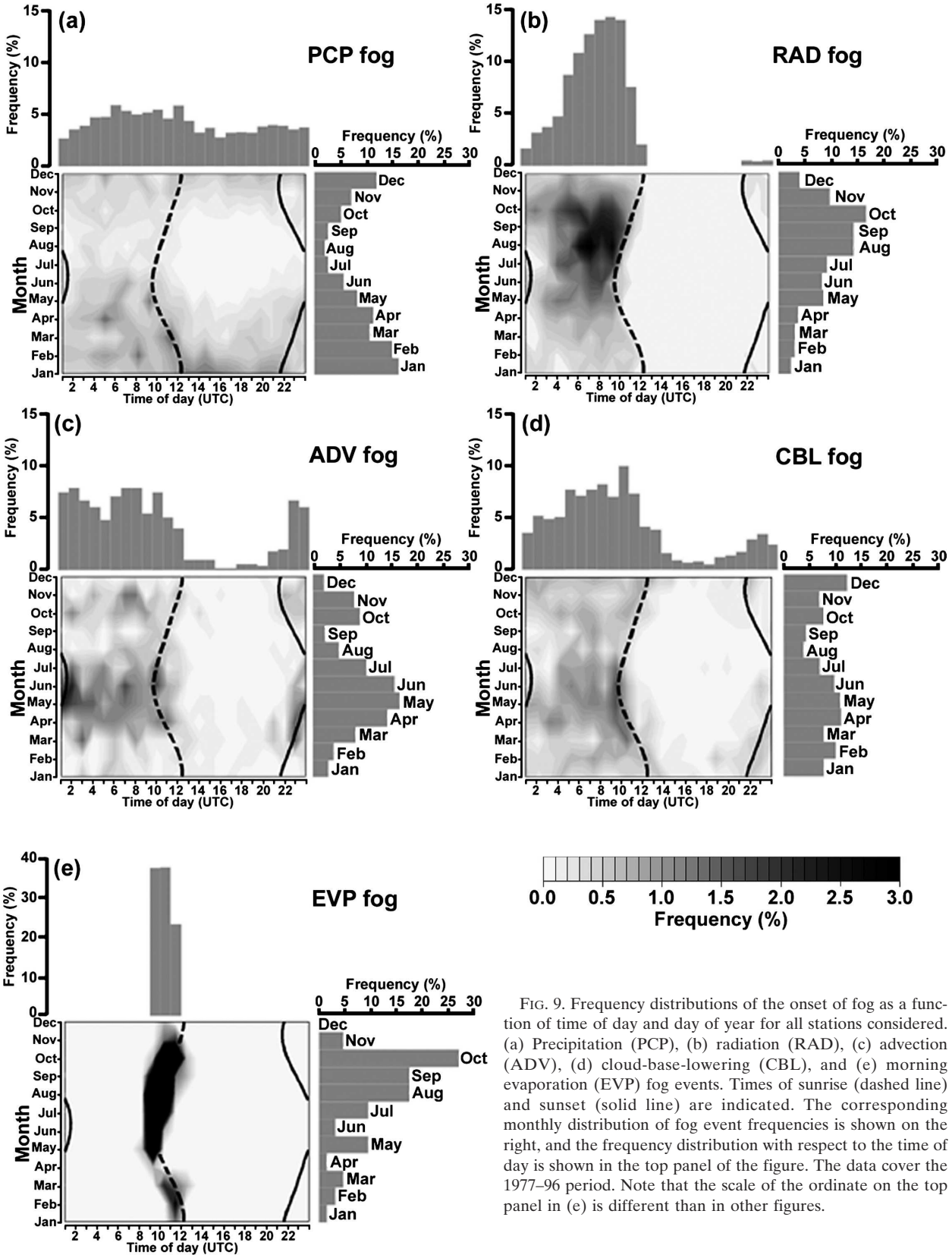

FIG. 9. Frequency distributions of the onset of fog as a function of time of day and day of year for all stations considered. (a) Precipitation (PCP), (b) radiation (RAD), (c) advection (ADV), (d) cloud-base-lowering (CBL), and (e) morning evaporation (EVP) fog events. Times of sunrise (dashed line) and sunset (solid line) are indicated. The corresponding monthly distribution of fog event frequencies is shown on the right, and the frequency distribution with respect to the time of day is shown in the top panel of the figure. The data cover the 1977–96 period. Note that the scale of the ordinate on the top panel in (e) is different than in other figures.

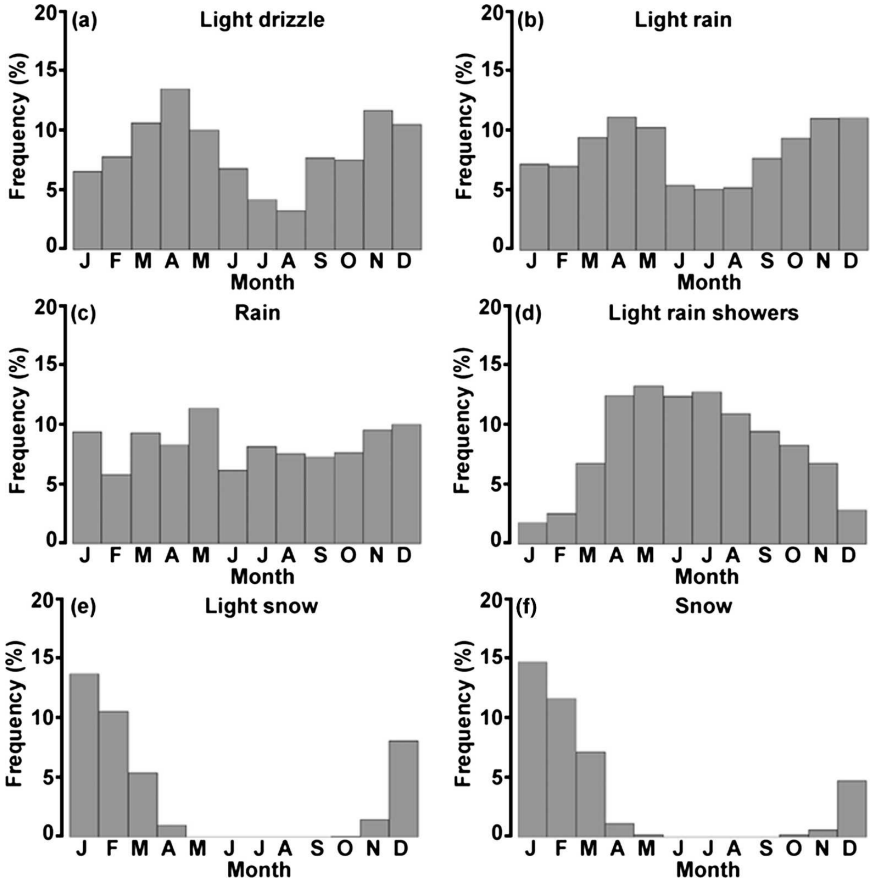

FIG. 10. Monthly frequency distributions of the most common precipitation categories in the New York City region: (a) light drizzle, (b) light rain, (c) rain, (d) light rain showers, (e) light snow, and (f) snow.

maximum likelihood occurring during winter. A gradual decrease in frequency characterizes the spring and early summer period (March–June), with a minimum in the distribution characterizing the midsummer to early autumn period (July–September). A ramp up in precipitation fog frequency occurs during October and November. This distribution shows some relation to the seasonal variability of light stratiform precipitation occurrences (Fig. 10) associated with the seasonal peak in cyclonic activity in the northeastern United States (Bell and Bosart 1989). This dependence on large-scale factors also supports the finding that a greater proportion of precipitation fog onset takes place during the daylight hours relative to other fog types, because factors associated to the diurnal cycle of the boundary layer do not appear to be as dominant as with other fog types (see below).

The temporal distribution of radiation fog indicates that events occur mostly in late summer (August) and autumn (September and October) (Fig. 9b). Some events occur in late spring and summer (May–July) and in November. The minimum frequency is found in winter and early spring (December–April). Radiation fog events tend to begin during the second half of the night. This is clearly evident during August and September. However, a larger proportion of events begins earlier in the night during the peak in October and during May and November. These results exhibit similar characteristics as those of Meyer and Lala (1990) for a location in the Hudson Valley about 220 km north of NYC. These authors indicate that such a seasonal distribution is determined by a superposition of the cooling potential (length of night) and moisture availability.

The monthly frequency of advection fog shows a bimodal distribution, with a marked peak during spring and early summer (April, May, and June) and a secondary maximum in the autumn (October and November) (Fig. 9c). Frequencies are minimized in winter (December, January, and February) and during late summer and early autumn (August and September). The spring maximum corresponds to the period of the year during which the offshore water temperature in-

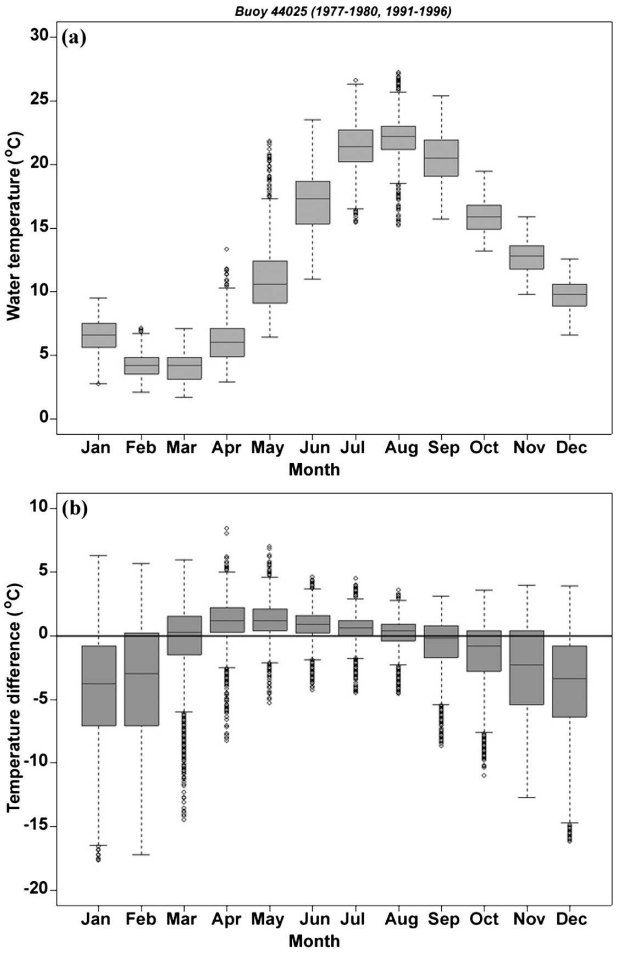

FIG. 11. Box plots illustrating the seasonal variability in the monthly distributions of the (a) sea surface temperature and (b) difference between the near-surface air temperature and the sea surface temperature (T_{air} − SST), at the 44025 buoy located south of Long Island. Data were provided by the National Data Buoy Center.

creases (Fig. 11a), but more importantly it is also the period when near-surface air temperatures a few degrees warmer than the sea surface temperature are observed more frequently (Fig. 11b). This is the typical scenario leading to sea (advection) fog defined by moist airstreams flowing over ocean surfaces, which are colder by a few degrees (Taylor 1917; Klein and Hartmann 1993; Roach 1995b; Cho et al. 2000). Similar conditions also characterize events during the autumn, but occurrences of such temperature contrasts between the low-level air and the water surface are not as frequent. On a diurnal time scale, advection fog onset occurs mostly during nighttime hours. The maximum likelihood of fog onset during the spring is right after sunset, complemented by significant frequencies throughout the rest of the night. During the secondary maximum in the autumn, the maximum is in the middle part of the night (between 0600 and 0800 UTC). During the daytime, the inland propagation of a coastal fog layer is determined by competing influences associated with solar warming of the landmass. The differential heating between the landmass and the ocean enhances the inland advection of sea fog through the generation of a sea-breeze circulation. At the same time, the solar warming over land leads to a dissipation of the fog by the convectively driven mixing of warm, dry air with the advancing marine layer. The result is often a marine fog that remains stationary in the vicinity of the coast. With decreasing solar radiation in the evening, the nighttime land surface temperature cools with an associated reduction of the turbulent mixing as a stable layer establishes itself over land. A cooler and less turbulent boundary layer allows an inland propagation of the fog layer under the influence of an onshore push either from the remnants of the sea breeze or from a synoptically driven circulation. This scenario is a plausible explanation for the maximum frequencies of fog onset at coastal land stations during the night.

The clear majority of fog events resulting from the lowering of the cloud base begin during the nighttime hours (Fig. 9d). The monthly distribution of this type of event shows somewhat less variability than for the other fog types. Nevertheless, an absolute maximum in the monthly frequencies takes place in December, with a secondary maximum observed during spring and early summer (April–June). The minimum frequencies take place during August and September. In examining the distribution of $F_{m,h}$, it is found that the onset of cloud-base-lowering fog is most likely to occur late during the night from March to July, with fewer events beginning earlier in the night. In April and May, some events begin just a few hours after sunset. During the peak in December, fog onset is distributed more evenly throughout the night. The reasons behind such behavior remain unclear without a more detailed investigation. However, similarities with advection and precipitation fog suggest that cooling of the boundary layer could be an important process leading to events in the spring, while events in winter could be associated with large-scale weather systems.

The monthly distribution of morning evaporation fog events shows a maximum likelihood during the period from August to October (Fig. 9e). This is very similar to the distribution exhibited by radiation fog events. This suggests that these events tend to occur on mornings following nights on which conditions were such that radiation fog did not form, likely under the influence of dew deposition. Studies have highlighted the role of dew deposition in controlling the onset of radiation fog

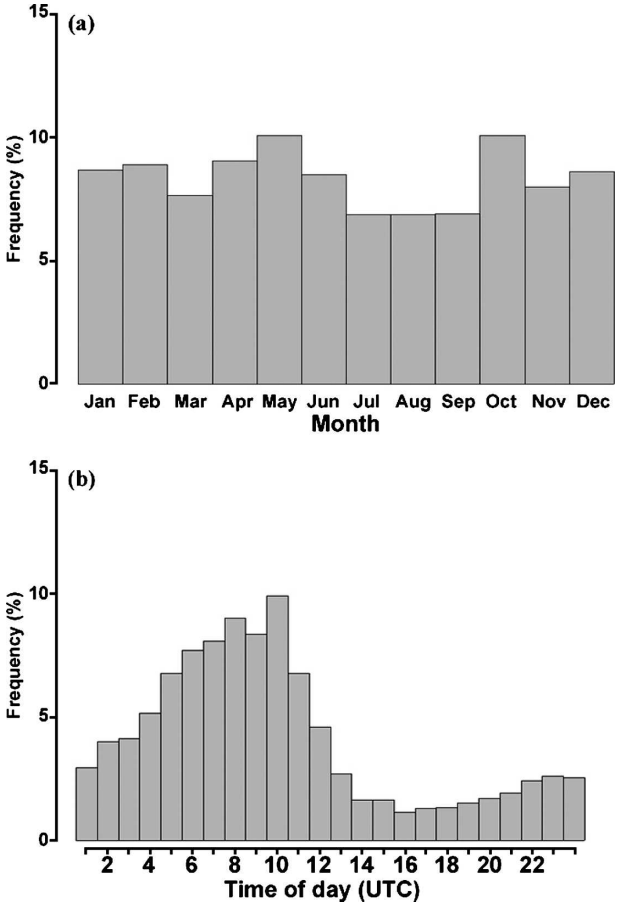

FIG. 12. (a) Monthly frequency distribution of all fog events and (b) diurnal frequency of fog onset, regardless of the fog type.

(Lala et al. 1975; Brown and Roach 1976; Pickering and Jiusto 1978; Bergot and Guédalia 1994). The water deposited on the surface during the night is readily available for evaporation once the incoming solar radiation provides the necessary energy after sunrise. The related influx of water vapor and mixing in the surface layer can lead to fog formation.

The superposition of fog types leads to fog events being distributed throughout the year, with a slight tendency for May and October to have the highest frequencies and the period from July to September to have the lowest (Fig. 12a). This is in overall agreement with the analysis presented by Hardwick (1973). With respect to the diurnal distribution of the time of fog onset, an overall tendency for fog to form during the second half of the night is clearly identified (Fig. 12b).

d. Diurnal variability of fog dissipation

The distribution of the timing of fog dissipation for each fog type is shown in Fig. 13. A distinct pattern is observed, showing a tendency for dissipation to occur 1–4 h after sunrise. In fact, an examination of conditions observed around the time of the termination of all events reveals that 72% are characterized by a decrease in relative humidity associated with increasing temperatures within a few hours after sunrise, and that 20% are characterized by a change to a drier air mass associated with a shift in wind direction. As for onset, precipitation fog is the type with the least dependence on the diurnal cycle. This suggests a greater proportion of events end because of influences other than solar heating, such as a shift in the low-level flow advecting drier air from the north as low pressure systems exit the region. This scenario is similar to observations made by George (1940) for Atlanta, Georgia, in the southeastern United States. The typical scenario for the dissipation of cloud-base-lowering and advection fogs is through the influence of increasing solar radiation, although a good fraction of events end during the night, likely under the influence of changing low-level horizontal advection during evolving synoptic conditions. The clear majority of radiation fogs dissipate within 1–4 h of sunrise under the influence of solar heating and increasing turbulent mixing (commonly referred to as "burn off"). This is in agreement with the results of Meyer and Lala (1990). Consistent with the previous findings on fog duration, the burn off of morning evaporation fog occurs only a few hours after onset.

e. Regional variability in relation to fog types

In contrast to previous studies aiming to describe the fog phenomenon at the continental scale (Peace 1969; Hardwick 1973) or for a single location (Meyer and Lala 1990), the present study resulted in the identification of a considerable small-scale spatial variability in fog character. Both common and contrasting features are found among coastal, inland, urban, and suburban or rural sites in terms of the relationship between fog types and the seasonal distribution of fog (Fig. 14). Overall, coastal sites experience precipitation, cloud-base lowering, and advection fog, while radiation fog is more prevalent at inland suburban and rural sites rather than advection fog. This leads to distinct features in the seasonal distribution of fog as suggested by results shown earlier in section 4c. For example, the fog maximum during spring at coastal locations (JFK, ISP, BDR, and LGA) is the result of a superposition of precipitation, cloud-base lowering, and advection fog. The maximum in autumn and winter at suburban and rural inland locations (BDL, POU, ABE, PNE, and ILG) is dominated by radiation fog in the autumn and is mostly composed of precipitation and cloud-base-lowering events during winter. The prevalence of radia-

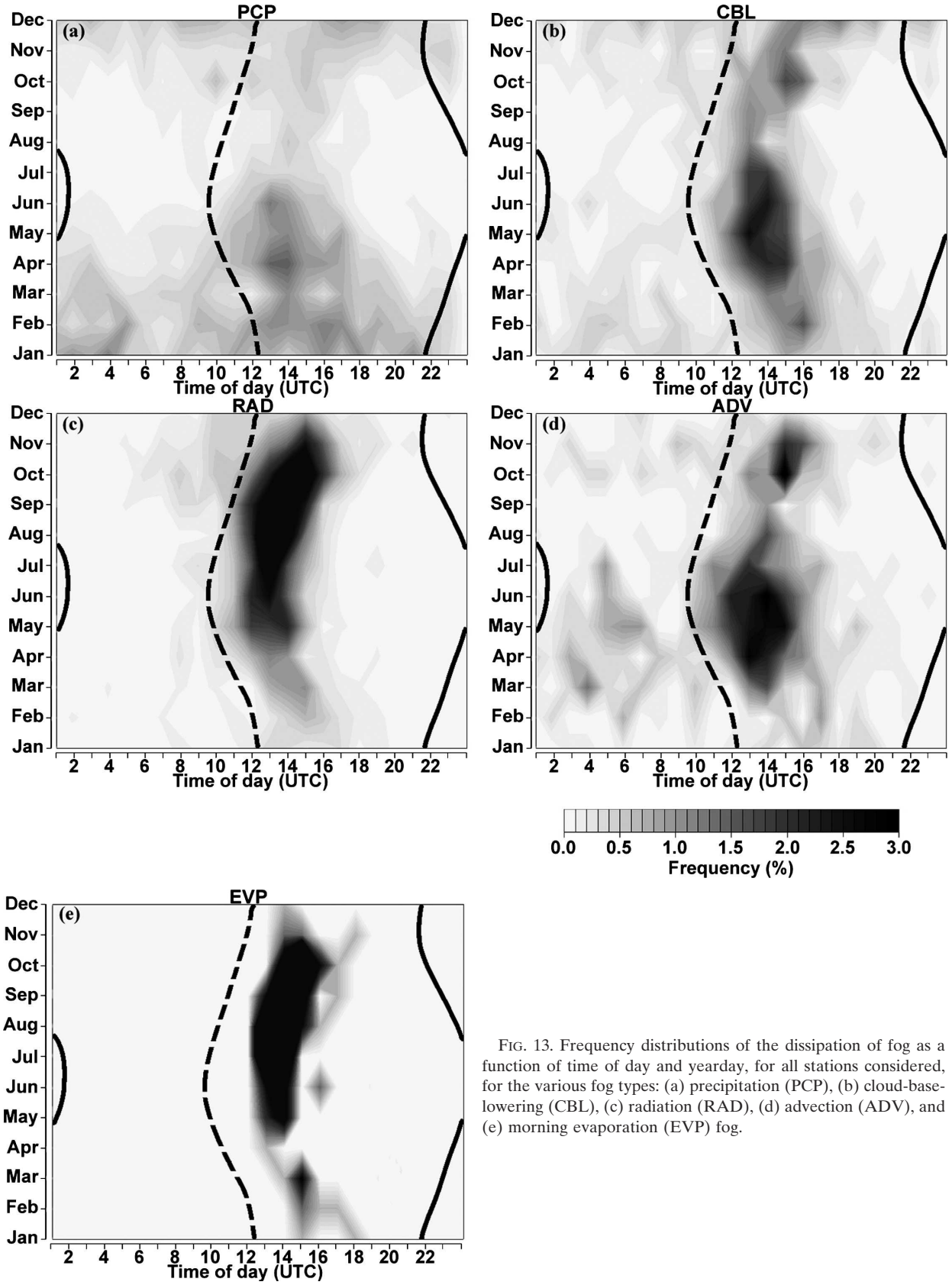

FIG. 13. Frequency distributions of the dissipation of fog as a function of time of day and yearday, for all stations considered, for the various fog types: (a) precipitation (PCP), (b) cloud-base-lowering (CBL), (c) radiation (RAD), (d) advection (ADV), and (e) morning evaporation (EVP) fog.

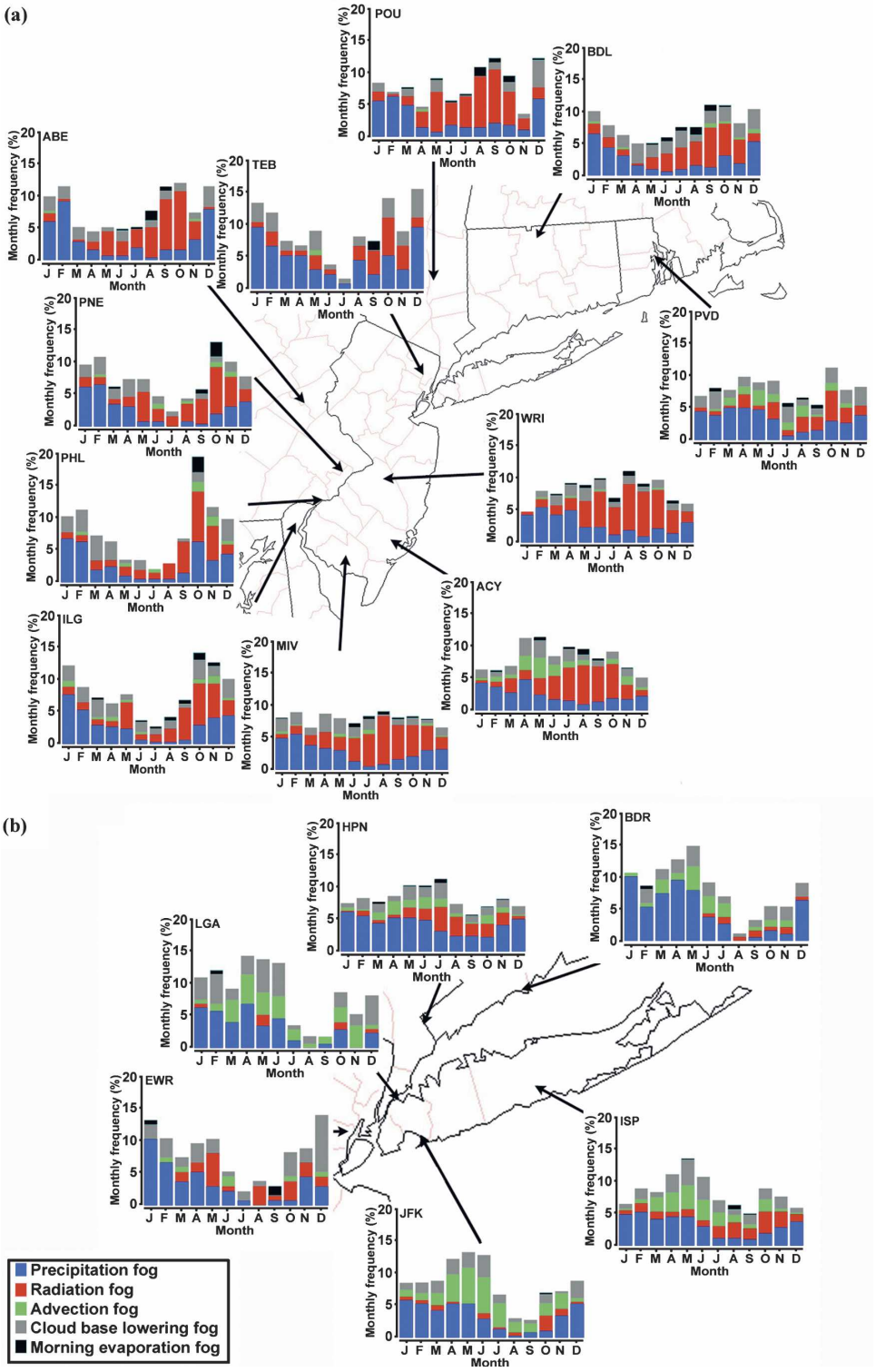

FIG. 14. (a) Monthly frequency distribution of fog types identified at sites in the New York City region. The monthly frequency of each fog type is represented by the height of bars with the corresponding color (see legend). The overall frequency is represented by the sum of each fog type (total height of bars). (b) Same as (a), but for locations within and in the general vicinity of the New York metropolitan area.

tion fog at POU is in accord with the findings of Meyer and Lala (1990) for Albany, New York, located 125 km to the north (also in the Hudson Valley).

The complexity of fog in the region is exacerbated by the fact that some sites exhibit contrasting characteristics. Events at coastal PVD occur most frequently in October through the combined influences of radiation, precipitation, and cloud-base-lowering events. Significant frequencies also characterize the winter and spring seasons with precipitation and cloud-base-lowering events occurring most frequently, along with a contribution from advection and radiation fogs in spring. Thus, in essence, this coastal site (next to Narragansett Bay) exhibits characteristics akin to both coastal and inland fog regimes.

Stations on the coastal plain of New Jersey (WRI, MIV, and ACY) have a greater number of events during the summer season, which translates into a weaker seasonal variability in the frequency of fog. This is the result of a greater number of radiation fog events during the warm season. Not surprisingly, the distribution at ACY also shows a coastal signature with a maximum in middle to late spring resulting from an enhanced likelihood of advection fog events. The monthly frequency distribution for HPN shows a significant amount of fog events occurring during summer resulting from a greater number of radiation and precipitation fog events than at nearby locations.

Considerable variability exists in the vicinity of urban centers. The number of events at urban NYC locations (EWR, TEB, and LGA) corresponds to 20%–50% of those at surrounding locations. Despite this contrast in overall fog likelihood, frequencies of precipitation and cloud-base-lowering fogs are maximized during late autumn, winter, and early spring within the urban core, which is the same as for the surrounding stations. Other fog types exhibit a greater level of variability in the vicinity of the urban core. Radiation fog is observed at EWR, TEB, ISP, and HPN, but is seldom encountered at JFK and LGA. The former stations are surrounded by a landmass for the most part, which offers some potential for nocturnal cooling. This is particularly the case at ISP and HPN, which are situated in suburban and rural areas, respectively. EWR and TEB are within a more heavily urbanized area, but Newark Bay and the wetlands surrounding the Hackensack River (patch of nonurban area between EWR and TEB in Fig. 1) represent local sources of moisture, which may influence the frequency of radiation fog. LGA is surrounded by a landmass except for a narrow opening on the Long Island Sound to the northeast. The surrounding landmass is characterized by a high-density urban surface where the maximum of the urban heat island is typically located (Gedzelman et al. 2003), thus minimizing the likelihood of radiation fog. Similar reasoning applies to the lack of radiation fog at JFK. Despite the moist environment resulting from the Atlantic Ocean, the effects of the UHI seem to dominate. The urban contrast is also present, but to a lesser extent at PHL. In contrast to NYC, PHL has a maximum in October whereas EWR and TEB have a local maximum in May, both resulting from an enhanced frequency of radiation fog.

5. Discussion

The shaping of the fog climatology through a superposition of different fog types is in general agreement with findings for other areas of the United States (George 1940; Byers 1959; Petterssen 1969; Croft et al. 1997; Baars et al. 2003) and the world (Bendix 2002; Cereceda et al. 2002). However, contrasts can be drawn between the NYC region and other coastal areas of the United States. The study of Croft et al. (1997) shows a distinct fog season from October to March for the coast of the Gulf of Mexico, with radiation and advection fogs being the dominant types. Baars et al. (2003) present results for the heavily urbanized coastal area of the Los Angeles, California, basin on the West Coast. Advection fog was found to be the dominant type, with advection–radiation fogs representing the only other significant type. This is complemented by a radiation fog regime in the central valley of California (Holets and Swanson 1981; Underwood et al. 2004). Very few precipitation fog events were identified. This is in contrast with the NYC region where precipitation fog is the most common type. Other accounts of common precipitation fog were reported by George (1940) for locations in the southeastern United States, with generally only one other distinct fog regime contributing significantly. Therefore, the fog phenomenon in NYC's region is composed of a superposition of a greater variety of fog types than some other regions in the United States.

The classification of fog events was based on the role of primary mechanisms leading to fog formation. However, the role of secondary mechanisms may be important as well. The maximum in events at HPN has been shown to be associated with a considerable contribution from precipitation fog. The low-level flows from the Long Island Sound at the onset of these events (Fig. 15), in association with a topography characterized by terrain sloping upward away from the coast, suggest that upslope flow may be a favorable secondary mechanism for fog formation (Tjernström 1993). As also pointed out by Willett (1944), supersaturation may be produced by the adiabatic cooling of air that has been saturated from rainfall evaporation.

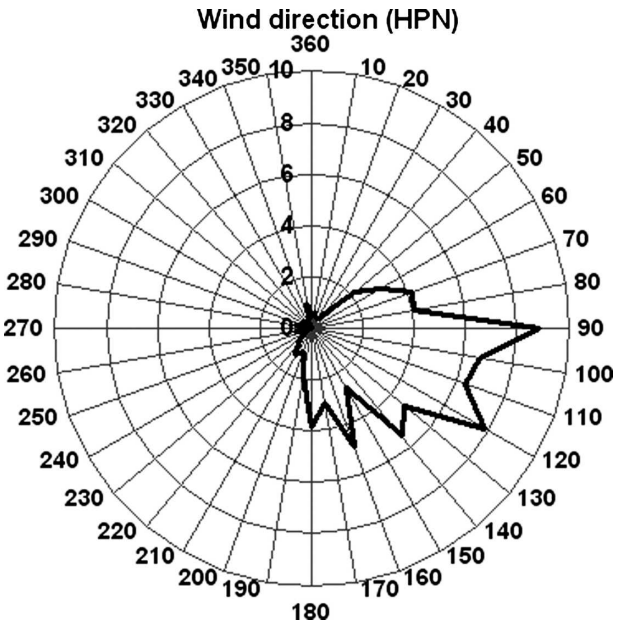

FIG. 15. Frequency of the wind direction observed at the onset of fog events at HPN.

Another noteworthy feature is the prevailing occurrence of radiation fog during the warm season on the coastal plain of New Jersey, and to some extent at HPN and POU. These events can be categorized as advection–radiation fog, in which moist air previously advected from the ocean is brought to saturation through radiative cooling over land (George 1951; Ryznar 1977). During the months of June, July, and August, the temperature of the coastal waters is at its peak (Fig. 11). A prevailing breeze from the south and southwest during the afternoon preceding foggy nights (Fig. 16) suggests that advection of moist air from the warm ocean under a sea-breeze circulation is responsible for keeping the dewpoints high over the coastal plain of New Jersey and the coastal areas of southern New York State. It is also suggested that the moist marine air may even reach POU. Despite the shorter nights in summer, saturation of the humid air mass may still be attained under the influence of significant nighttime radiative cooling in sandy soil regions. In such instances, the prior advection of moist air over land can be considered an important secondary mechanism.

As pointed out in the previous section, morning evaporation fog events tend to occur particularly at locations prone to radiation fog. This suggests that nights on which radiation fog did not quite form because of sufficient dehydration of the surface layer by the deposition of dew may, in fact, lead to conditions conducive to morning evaporation fog. This is supported by the finding that an average change in the specific humidity of -0.65 g kg^{-1} took place during the 6 h prior to sunrise in cases of morning evaporation fog events. This value roughly equates the increase in moisture observed at sunrise. Dew deposition during the night can be considered an important secondary mechanism preceding morning evaporation fog.

6. Conclusions

The motivation for this study was the identification of the general characters of fog in a complex coastal/urban region of the northeastern United States. Fog events were identified, and each was assigned a type using a simple classification algorithm based on the primary mechanisms responsible for the initial formation of fog. The character of each fog type was examined in terms of intensity (severity of visibility reduction) and duration as well as spatial and temporal variability. The results show the following:

1) A greater variety of fog types occurs in the NYC region relative to some other studied regions in the United States. The fog phenomenon in the region is a superposition of precipitation, cloud-base-lowering, advection, and radiation fog, with some events of morning evaporation fog. Dominant fog types have been identified in various parts of the region, yet appreciable frequencies characterize secondary and tertiary fog types. This represents a greater variety than that on the West and Gulf Coast regions of the United States, which is dominated by advection fogs along the coast and radiation fogs at inland locations. Other fog types affect other parts of the United States, but investigated sites are generally characterized by two types contributing significantly to the overall fog phenomenon.
2) Considerable intraregional variability in fog types is present in response to the complex physiographic character of the region. Advection fog events occur at coastal sites and are tied to positive temperature differences between the near-surface air and the sea surface itself. Such occurrences are maximized in spring. Radiation events are not only confined to the typical autumn season under the influence of cold-air pooling at inland valley locations, but also occur in the coastal plain during the warm season as advection–radiation events. Short-lived morning evaporation fogs occur at locations prone to radiation fog, following nights on which dew deposition contributed to limit the nocturnal formation of fog. Urban effects are clearly identified through the minimization of the total number of fog hours, fog days, and fog events at locations within and in the

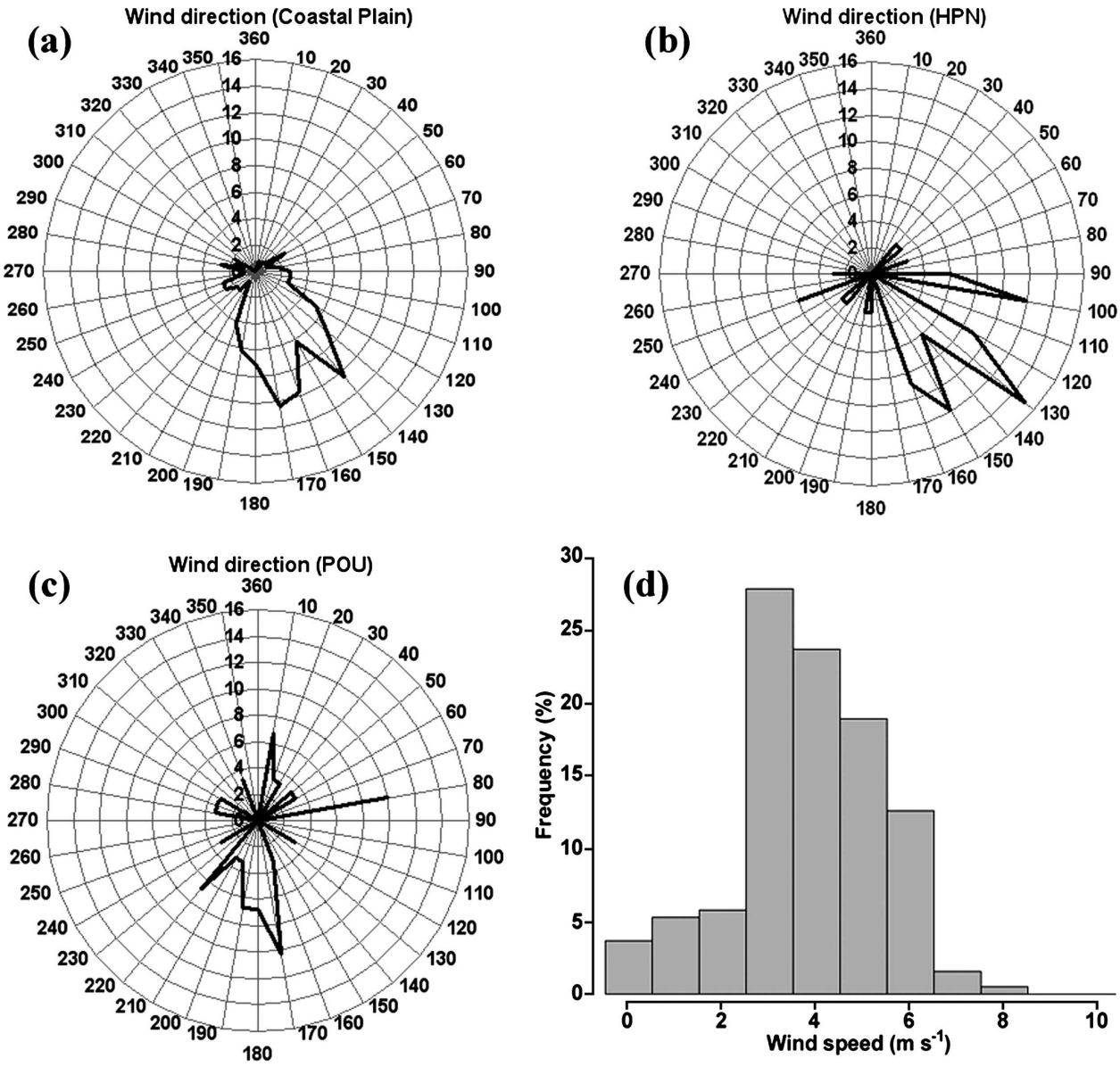

FIG. 16. Frequency of wind direction at stations in (a) the coastal plain of New Jersey (ACY, MIV, and WRI), (b) HPN, and (c) POU, as well as (d) the wind speed at all these stations observed during the afternoon preceding the occurrence of radiation fog during summer.

immediate vicinity of NYC and to a lesser extent Philadelphia. The stations with minimum fog correspond to the urban areas of the highest nocturnal temperatures shown by Gedzelman et al. (2003). Other types are less susceptible to surface characteristics. Cloud-base-lowering fog occurs throughout the region with enhanced frequencies in winter and spring, suggesting an association with synoptic-scale weather systems in winter and with changing conditions within the stratus-topped marine boundary layer in spring. Precipitation fog events are the most common throughout the region with a seasonal variability influenced by the annual cycle of stratiform precipitation (maximum in winter).

3) Fog types have characteristic duration and visibility reduction. Precipitation fog produces fewer heavy fog conditions than the radiation of advection fog. In contrast, the average precipitation fog event last the longest, followed by cloud-base-lowering, advection, radiation, and, finally, morning evaporation fog.
4) The dissipation of fog occurs mainly through the

burn-off process. While fog dissipation typically occurs a few hours after sunrise under the influence of rising temperatures and decreasing relative humidity (72% of the total number of events), some events (20%), particularly of the precipitation type, end at other times of the day under the influence of evolving synoptic weather conditions leading to a change to a drier air mass.

These results can serve as a basis for more detailed investigations of the various factors influencing the life cycle of fog in all of its forms. Classifying events into fog types sets the stage for a focused analysis of the environmental conditions (synoptic weather patterns, surface layer evolution, tropospheric vertical structure, etc.) associated with individual fog types. This will be the subject of future efforts. The accurate prediction of fog continues to be an elusive goal. We offer that the most hopeful approach to the fog forecasting problem consists of gaining a greater understanding of the various mechanisms involved in its formation, maintenance, and dissipation. The premise of our study is that information about important climatological parameters can serve as basic guidance on the likelihood of fog formation and that such information can be beneficial to weather forecasters in their efforts to produce true forecasts rather than be forced to react once formation has occurred. The development of statistical methods and improved numerical model parameterizations based on a deeper understanding of the important physical processes should also lead to improved guidance from the next-generation forecast systems.

Acknowledgments. The authors thank Ben Bernstein of NCAR/RAL for providing an early version of the software used to analyze the surface observations. Thanks are given to Wes Wilson of NCAR/RAL for pointing out the existence of the *M*-of-*N* concept in the statistical literature. Many thanks are given to Dr. Thierry Bergot for his comments on an early version of the manuscript. The insightful comments of three anonymous reviewers contributed greatly to the improvement of the manuscript. This research is in response to requirements and funding by the Federal Aviation Administration (FAA). The views expressed are those of the author and do not necessarily represent the official policy or position of the FAA.

REFERENCES

Allan, S. S., S. G. Gaddy, and J. E. Evans, 2001: Delay causality and reduction at the New York City airports using terminal weather information systems. Massachusetts Institute of Technology, Lincoln Laboratory, Project Rep. ATC-291, 48 pp.

Arya, P. A., 2001: *Introduction to Micrometeorology*. 2d ed. Academic Press, 415 pp.

Baars, J. A., M. Witiw, and A. Al-Habash, 2003: Determining fog type in the Los Angeles basin using historic surface observation data. *Proc. 16th Conf. on Probability and Statistics in the Atmospheric Sciences,* Long Beach, CA, Amer. Meteor. Soc., CD-ROM, J3.8.

Baker, R., J. Cramer, and J. Peters, 2002: Radiation fog: UPS Airlines conceptual models and forecast methods. *Proc. 10th Conf. on Aviation, Range and Aerospace Meteorology,* Portland, OR, Amer. Meteor. Soc., 154–159.

Ballard, S. P., B. W. Golding, and R. N. B. Smith, 1991: Mesoscale model experimental forecasts of the haar of northeast Scotland. *Mon. Wea. Rev.,* **119,** 2107–2123.

Bell, G. D., and L. F. Bosart, 1989: A 15-year climatology of Northern Hemisphere 500 mb closed cyclone and anticyclone centers. *Mon. Wea. Rev.,* **117,** 2142–2163.

Bendix, J., 1994: Fog climatology of the Po Valley. *Riv. Meteor. Aeronaut.,* **54** (3–4), 25–36.

——, 2002: A satellite-based climatology of fog and low-level stratus in Germany and adjacent areas. *Atmos. Res.,* **64,** 3–18.

Bergot, T., and D. Guédalia, 1994: Numerical forecasting of radiation fog. Part I: Numerical model and sensitivity tests. *Mon. Wea. Rev.,* **122,** 1218–1230.

Bornstein, R. D., 1968: Observations of the urban heat island effect in New York City. *J. Appl. Meteor.,* **7,** 575–582.

Bott, A., 1991: On the influence of the physico-chemical properties of aerosols on the life cycle of radiation fogs. *Bound.-Layer Meteor.,* **56,** 1–31.

Brown, R., and W. T. Roach, 1976: The physics of radiation fog, Part II: A numerical study. *Quart. J. Roy. Meteor. Soc.,* **102,** 335–354.

Brutsaert, W. H., 1982: *Evaporation into the Atmosphere*. D. Reidel, 299 pp.

Byers, H. R., 1959: *General Meteorology*. McGraw-Hill, 481 pp.

Cereceda, P., P. Osses, H. Larrain, M. Farías, M. Lagos, R. Pinto, and R. J. Schemenauer, 2002: Advective, orographic and radiation fog in the Tarapacá region, Chile. *Atmos. Res.,* **64,** 261–271.

Cho, Y.-K., M.-O. Kim, and B.-C. Kim, 2000: Sea fog around the Korean peninsula. *J. Appl. Meteor.,* **39,** 2473–2479.

Choularton, T. W., G. Fullarton, J. Latham, C. S. Mill, M. H. Smith, and I. M. Stromberg, 1981: A field study of radiation fog in Meppen, West Germany. *Quart. J. Roy. Meteor. Soc.,* **107,** 381–394.

Croft, P. J., 2003: Fog. *Encyclopedia of Atmospheric Sciences,* J. R. Holton, J. A. Curry, and J. A. Pyle, Eds., Academic Press, 777–792.

——, and A. N. Burton, 2006: Fog during the 2004–2005 winter season in the northern mid-Atlantic states: Spatial characteristics and behaviors as a function of synoptic weather types. *Proc. 12th Conf. on Aviation, Range and Aerospace Meteorology,* Atlanta, GA, Amer. Meteor. Soc., CD-ROM, P3.3.

——, R. L. Pfost, J. M. Medlin, and G. A. Johnson, 1997: Fog forecasting for the southern region: A conceptual model approach. *Wea. Forecasting,* **12,** 545–556.

Duynkerke, P. G., 1991: Observation of a quasi-periodic oscillation due to gravity waves in a shallow fog layer. *Quart. J. Roy. Meteor. Soc.,* **117,** 1207–1224.

——, and P. Hignett, 1993: Simulation of diurnal variation in a stratocumulus-capped marine boundary layer during FIRE. *Mon. Wea. Rev.,* **121,** 3291–3300.

Findlater, J., W. T. Roach, and B. C. McHugh, 1989: The haar of north-east Scotland. *Quart. J. Roy. Meteor. Soc.,* **115,** 581–608.

Fitzjarrald, D. R., and G. G. Lala, 1989: Hudson Valley fog environments. *J. Appl. Meteor.,* **28,** 1303–1328.

Friedlein, M. T., 2004: Dense fog climatology: Chicago O'Hare International Airport, July 1996–April 2002. *Bull. Amer. Meteor. Soc.,* **85,** 515–517.

Fuzzi, S., and Coauthors, 1998: Overview of the Po Valley fog experiment 1994 (CHEMDROP). *Contr. Atmos. Phys.,* **71,** 3–19.

Gedzelman, S. D., S. Austin, R. Cermak, N. Stefano, S. Partridge, S. Quesenberry, and D. A. Robinson, 2003: Mesoscale aspects of the urban heat island around New York City. *Theor. Appl. Climatol.,* **75,** 29–42.

George, J. J., 1940: Fog: Its causes and forecasting with special reference to eastern and southern United States. *Bull. Amer. Meteor. Soc.,* **21,** 135–148, 261–269, 285–291.

——, 1951: Fog. *Compendium of Meteorology,* T. F. Malone, Ed. Amer. Meteor. Soc., 1179–1189.

Golding, B. W., 1993: A study of the influence of terrain on fog development. *Mon. Wea. Rev.,* **121,** 2529–2541.

Goodman, J., 1977: The microstructure of California coastal fog and stratus. *J. Appl. Meteor.,* **16,** 1056–1067.

Hardwick, W. C., 1973: Monthly fog frequency in the continental United States. *Mon. Wea. Rev.,* **101,** 763–766.

Helsel, D. R., and R. M. Hirsch, 1992: *Statistical Methods in Water Resources.* Vol. 49, *Studies in Environmental Science,* Elsevier, 529 pp.

Holets, S., and R. N. Swanson, 1981: High-inversion fog episodes in central California. *J. Appl. Meteor.,* **20,** 890–899.

Hudson, J. G., 1980: Relationship between fog condensation nuclei and fog microstructure. *J. Atmos. Sci.,* **37,** 1854–1867.

Ito, K., N. Xue, and G. Thurston, 2004: Spatial variation of $PM_{2.5}$ chemical species and source-apportioned mass concentrations in New York City. *Atmos. Environ.,* **38,** 5269–5282.

Klein, S. A., and D. L. Hartmann, 1993: The seasonal cycle of low stratiform clouds. *J. Climate,* **6,** 1587–1606.

Koračin, D., J. Lewis, W. T. Thompson, C. E. Dorman, and J. A. Businger, 2001: Transition of stratus into fog along the California coast: Observations and modeling. *J. Atmos. Sci.,* **58,** 1714–1731.

——, J. A. Businger, C. E. Dorman, and J. M. Lewis, 2005: Formation, evolution, and dissipation of coastal sea fog. *Bound.-Layer Meteor.,* **117,** 447–478.

LaDochy, S., 2005: The disappearance of dense fog in Los Angeles: Another urban impact*? Phys. Geogr.,* **26,** 177–191.

Lala, G. G., E. Mandel, and J. E. Jiusto, 1975: Numerical evaluation of radiation fog variables. *J. Atmos. Sci.,* **32,** 720–728.

Lee, T. F., 1987: Urban clear islands in California central valley fog. *Mon. Wea. Rev.,* **115,** 1794–1796.

Leipper, D. F., 1994: Fog on the U.S. west coast: A review. *Bull. Amer. Meteor. Soc.,* **75,** 229–240.

Lewis, J., D. Koracin, R. Rabin, and J. Businger, 2003: Sea fog off the California coast: Viewed in the context of transient weather systems. *J. Geophys. Res.,* **108,** 4457, doi:10.1029/2002JD002833.

Meyer, M. B., and G. G. Lala, 1990: Climatological aspects of radiation fog occurrence at Albany, New York. *J. Climate,* **3,** 577–586.

——, ——, and J. E. Jiusto, 1986: FOG-82: A cooperative field study of radiation fog. *Bull. Amer. Meteor. Soc.,* **67,** 825–832.

Nakanishi, M., 2000: Large-eddy simulation of radiation fog. *Bound.-Layer Meteor.,* **94,** 461–493.

National Center for Atmospheric Research, cited 2006: TDL U.S. and Canada surface hourly observations, daily 1976Dec-cont. [Available online at http://dss.ucar.edu/datasets/ds472.0/.]

National Oceanic and Atmospheric Administration, 1995: Surface weather observations and reports. Federal Meteorological Handbook 1, 94 pp.

National Weather Service, Aviation Services Branch, 2004: Terminal aerodrome forecasts. NWS Instruction 10-813, 57 pp.

Oliver, D. A., W. S. Lewellen, and G. G. Williamson, 1978: The interaction between turbulent and radiative transport in the development of fog and low-level stratus. *J. Atmos. Sci.,* **35,** 301–316.

Pagowski, M., I. Gultepe, and P. King, 2004: Analysis and simulation of an extremely dense fog event in southern Ontario. *J. Appl. Meteor.,* **43,** 3–16.

Peace, R. L., 1969: Heavy fog regions in the conterminous United States. *Mon. Wea. Rev.,* **97,** 116–123.

Peak, J. E., and P. M. Tag, 1989: An expert system approach for prediction of maritime visibility obscuration. *Mon. Wea. Rev.,* **117,** 2641–2653.

Petterssen, S., 1940: *Weather Analysis and Forecasting*. McGraw-Hill, 505 pp.

——, 1969: *Introduction to Meteorology*. 3d ed. McGraw-Hill, 333 pp.

Pickering, K. E., and J. E. Jiusto, 1978: Observations of the relationship between dew and radiation fog. *J. Geophys. Res.,* **83,** 2430–2436.

Pilié, R. J., E. J. Mack, W. C. Kocmond, C. W. Rogers, and W. J. Eadie, 1975: The life cycle of valley fog. Part I: Micrometeorological characteristics. *J. Appl. Meteor.,* **14,** 347–363.

——, ——, C. W. Rogers, U. Katz, and W. C. Kocmond, 1979: The formation of marine fog and the development of fog-stratus systems along the California coast. *J. Appl. Meteor.,* **18,** 1275–1286.

Roach, W., 1995a: Back to basics: Fog: Part 2 – The formation and dissipation of land fog. *Weather,* **50,** 7–11.

——, 1995b: Back to basics: Fog: Part 3 – The formation and dissipation of sea fog. *Weather,* **50,** 80–84.

——, R. Brown, S. J. Caughey, J. A. Garland, and C. J. Readings, 1976: The physics of radiation fog: I – A field study. *Quart. J. Roy. Meteor. Soc.,* **102,** 313–333.

Ryznar, E., 1977: Advection-radiation fog near Lake Michigan. *Atmos. Environ.,* **11,** 427–430.

Sachweh, M., and P. Koepke, 1995: Radiation fog and urban climate. *Geophys. Res. Lett.,* **22,** 1073–1076.

——, and ——, 1997: Fog dynamics in an urbanized area. *Theor. Appl. Climatol.,* **58,** 87–93.

Setiono, R., S.-L. Pan, M.-H. Hsieh, and A. Azcarraga, 2005: Automatic knowledge extraction from survey data: Learning M-of-N constructs using a hybrid approach. *J. Oper. Res. Soc. Amer.,* **56,** 3–14.

Taylor, G. I., 1917: The formation of fog and mist. *Quart. J. Roy. Meteor. Soc.,* **43,** 241–268.

Teixeira, J., 1999: Simulation of fog with the ECMWF prognostic cloud scheme. *Quart. J. Roy. Meteor. Soc.,* **125,** 529–552.

Thompson, W. T., S. D. Burk, and J. Lewis, 2005: Fog and low clouds in a coastally trapped disturbance. *J. Geophys. Res.,* **110,** D18213, doi:10.1029/2004JD005522.

Tjernström, M., 1993: Simulated water content and visibility in stratiform boundary-layer clouds over sloping terrain. *J. Appl. Meteor.,* **32,** 656–665.

Turton, J. D., and R. Brown, 1987: A comparison of a numerical model of radiation fog with detailed observations. *Quart. J. Roy. Meteor. Soc.,* **113,** 37–54.

Underwood, S. J., G. P. Ellrod, and A. L. Kuhnert, 2004: A multiple-case analysis of nocturnal radiation-fog development in the Central Valley of California utilizing the GOES nighttime fog product. *J. Appl. Meteor.,* **43,** 297–311.

Valdez, J., 2000: National Weather Service—A high impact agency . . . *we make a difference:* Reinvention goals for 2000. National Weather Service. [Available online at http://govinfo.library.unt.edu/npr/library/announc/npr5.htm.]

Westcott, N., 2004: Synoptic conditions associated with dense fog in the Midwest. *Proc. 14th Conf. on Applied Climatology,* Seattle, WA, Amer. Meteor. Soc., CD-ROM, P2.4.

Whiffen, B., 2001: Fog: Impact on aviation and goals for meteorological prediction. *Proc. Second Conf. on Fog and Fog Collection,* St. John's, NF, Canada, Environment Canada and International Development Research Center, 525–528.

——, P. Delannoy, and S. Siok, 2003: Fog: Impact on road transportation and mitigation options. *Proc. 10th World Congress and Exhibition on Intelligent Transportation Systems and Services,* Madrid, Spain.

Willett, H. C., 1928: Fog and haze, their causes, distribution, and forecasting. *Mon. Wea. Rev.,* **56,** 435–468.

——, 1944: *Descriptive Meteorology*. Academic Press, 310 pp.

Wilson, F. W., and D. A. Clark, 1997: Estimation of the avoidable cost of ceiling and visibility events at major airports. *Proc. Seventh Conf. on Aviation, Range and Aerospace Meteorology,* Long Beach, CA, Amer. Meteor. Soc., 480–485.